

TEM and STEM Image Simulation

Winter School on High Resolution Electron Microscopy

Held at the

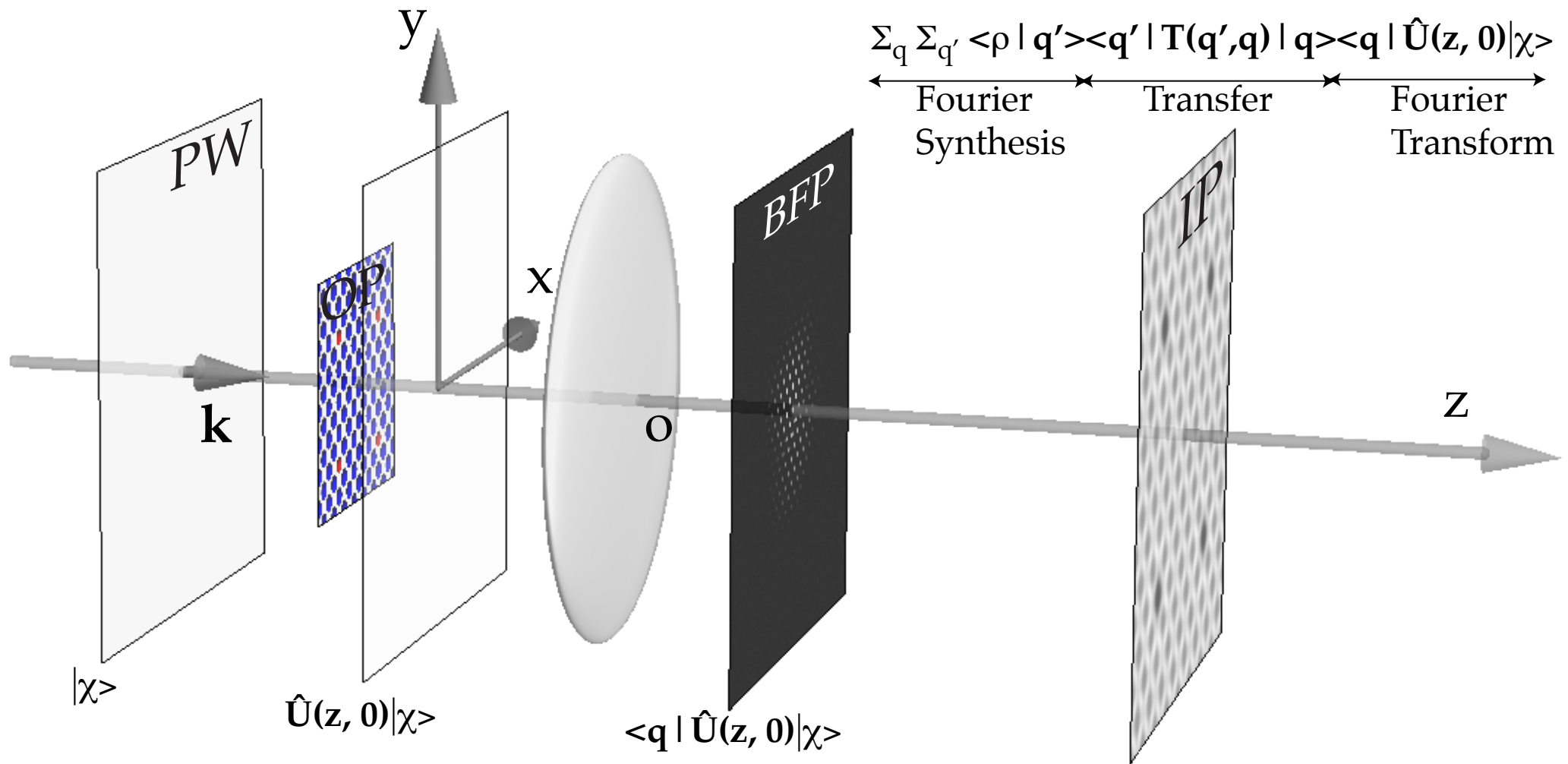
John M. Cowley Center for High Resolution Electron Microscopy

January 5 - 10, 2020

Pierre Stadelmann
JEMS-SWISS
CH-1805 Jongny
Switzerland

December 20, 2019

TEM: reminder



TEM modelling steps: incident wave (PW), crystal (OP), electron-matter interaction, Fraunhofer approximation, image formation (Abbe theory), ...

- —→ **Dynamical scattering.**
- Optical system.
- Comparing HRTEM and HRSTEM.

$|\chi\rangle \implies$ incident wave-function

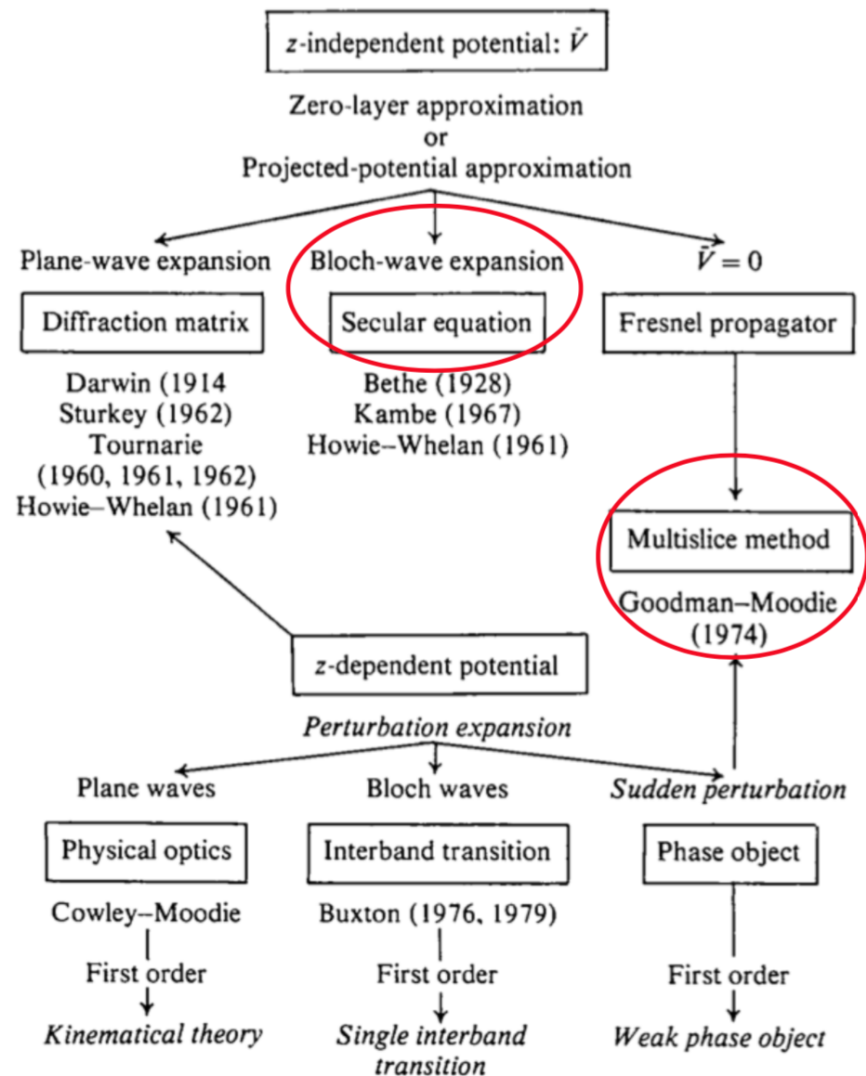
$|\psi_i\rangle \implies$ image wave-function

$$|\Psi_i\rangle = \underbrace{\sum_{q'} \langle \rho | q' \rangle}_{\text{Fourier synthesis}} \underbrace{\sum_q \langle q' | \hat{T}(q', q) | q \rangle}_{\text{Objective lens transfer}} \underbrace{\langle q | \hat{U}(z, 0) | \chi \rangle}_{\text{Fourier transform}}$$

$|\psi_i(\rho)|^2 \implies$ image intensity

(simple?) (complicated?) (mysterious?) formula of image formation in TEM?

$$H(z) = \frac{1}{2K} (-\nabla^2 - \chi^2 + V(z)) = H^0 + \frac{V(z)}{2K}$$



A few remarks to start

In the small angle approximation of electron diffraction the 3 dimensional stationary problem is replaced by a 2 dimensional problem where time is replaced by z .

- The electron microscope destroys the **space isotropy** as the electron are propagating **thousand times faster** in the direction defined by the **optical column** of the microscope (z direction) than in the plane perpendicular to it ($O_{x,y}$ plane).
- The **dynamical theory of elastic diffraction** calculates the amplitude and phase diffracted in a set of directions $\{|q\rangle\}$ selected by the **Bragg law**.
- Given a known initial state $|\chi\rangle$ (direction of incident electrons), what is the **transition probability** $\omega_{|\chi\rangle\rightarrow|q\rangle}$ after interaction with a scattering potential during **time z** (crystal thickness) to particular final state $|q\rangle$ (i.e. a diffracted beam).

The fundamental equation of the elastic diffraction of electrons in a potential V is given in the stationary mono-electronic approximation (constant electron flux, no energy dispersion) ²:

$$(\Delta + k^2)\Phi = V\Phi \quad (1)$$

where the wave vector k is $k = \frac{\sqrt{2meE}}{\hbar}$, m the mass of the electron corrected for relativistic effect $m = \gamma m_0$. The mean inner crystal potential $V_v(\vec{\rho}, z)$ is positive and of the order of 30 - 40 volts.

c = speed of light in vacuum.

e = electron charge.

E = accelerating voltage ($\geq 50kV$).

γ = $1 + \frac{e^2 E^2}{2 m_0 c^2}$ (relativistic mass correction).

m_0 = rest mass of the electron ($\approx 511 keV$).

V = $-\frac{2 m e}{\hbar^2} V_v(\vec{\rho}, z)$ (scattering potential [nm^{-2}]).

²C. Humphreys, *The scattering of fast electrons by crystals*, Reports on Progress in Physics Volume **42**, Number 11 (1979),1825.

E [kV]	γ	λ [pm]	$\frac{v}{c}$
50	1.098	5.362	0.412
100	1.119	3.706	0.548
200	1.391	2.511	0.695
500	1.978	1.423	0.862
1000	2.957	0.873	0.941

Relativistic mass correction γ , wavelength λ and speed of the electron

(hkl)	Bragg angle [mrad]	Bragg angle [deg.]	(hkl) spacing nm^{-1}
(1,1,1)	7.91	0.453	4.276
(2,0,0)	9.14	0.523	4.938
(2,2,0)	12.92	0.740	6.983
(1,1,3)	15.15	0.868	8.189
(2,2,2)	15.83	0.906	8.553
(4,0,0)	18.28	1.047	9.876

Bragg angles for some Al reflections at 100 kV.

The **small angle scattering** is a good approximation for electrons of 50 keV or larger. At very high energy Bragg angles are very small.

Elastic scattering

The electron microscope **destroys** the space isotropy because of the very high kinetic energy of the electrons. The 3-D space is thus described by $(\vec{\rho}, z)$ where $\vec{\rho} = (x, y)$.

Figure 1 shows the wave vectors \vec{k}_o and \vec{k}_q the incident beam and of a reflection respectively. They are both located on the Ewald sphere, i.e. the sphere of all possible direction of elastic scattering.

Elastic scattering: $\vec{k}_q = \vec{k}_o + \vec{q}$.

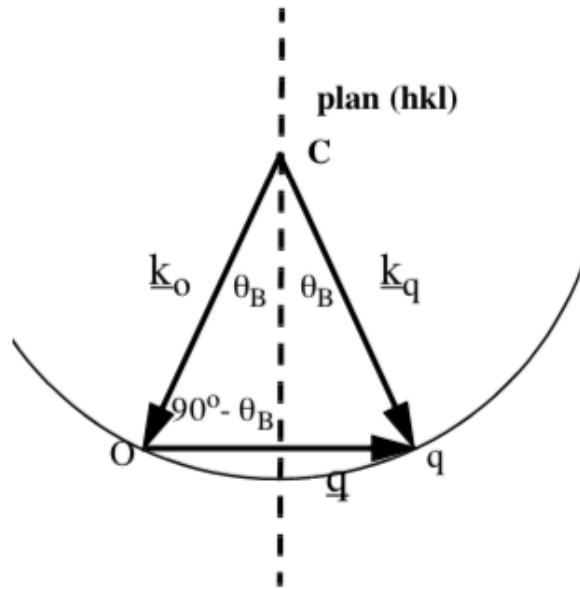


Figure: Elastic scattering.

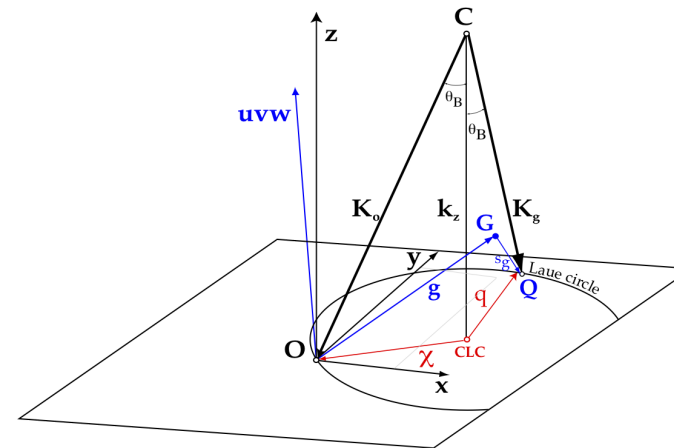


Figure: Diffraction Geometry.

Elastic scattering satisfies $|\vec{k}_q| = |\vec{k}_o|$ and $\vec{k}_q - \vec{q} = \vec{k}_o$. Combining these 2 equations:
 $2|\vec{k}_o| \cos\left(\frac{\pi}{2} - \theta_B\right) = |\vec{q}|$. **Bragg law:** $2d \sin \theta_B = \lambda$.

For a typical d of 10 nm^{-1} and wave vector of 400 nm^{-1} (at 200 kV), the Bragg angle is of the order of 0.15 degree. Thus the **small angle scattering approximation** is well verified in high energy transmission electron microscopy.

The geometry of the dynamical theory is defined in Figure 2. The wave vector \vec{k}_o of the incident electron is close to a $[u, v, w]$ crystal direction (zone axis): the miss-orientation is given by $\vec{\chi}$, projection of \vec{k}_o on the $O_{x,y}$ plane. The z component k_z of \vec{k}_o is very large (400 nm^{-1}). As a result the electron wave oscillates with a very high frequency in the z direction.

The **electron wave function** $\psi(\vec{\rho}, z)$ is written as:

$$\phi(\vec{r}) = \phi(\vec{\rho}, z) = e^{ik_z z} \psi(\vec{\rho}, z) \quad (2)$$

where $\psi(\vec{\rho}, z)$ is a **slowly varying** function of z. Putting (2) into $(\Delta + k^2)\Phi = V\Phi$ and neglecting $\frac{\partial^2}{\partial z^2}$ because:

$$\left| \frac{\partial \psi(\vec{\rho}, z)}{\partial z} \right| \gg \frac{1}{2k_z} \left| \frac{\partial^2 \psi(\vec{\rho}, z)}{\partial z^2} \right|$$

$$|\psi(\vec{\rho}, z)| \gg \frac{1}{2k_z} \left| \frac{\partial^2 \psi(\vec{\rho}, z)}{\partial z^2} \right|$$

$$i \frac{\partial}{\partial z} \psi(\vec{\rho}, z) = \frac{1}{2k_z} [-\Delta_\rho - \chi^2 + V(\vec{\rho}, z)] \psi(\vec{\rho}, z) \quad (3)$$

$$i\frac{\partial}{\partial z}\psi(\vec{\rho}, z) = \frac{1}{2k_z} [-\Delta_\rho - \chi^2 + V(\vec{\rho}, z)] \psi(\vec{\rho}, z) \quad (4)$$

- The approximations of the fundamental equation (4) is equivalent to assume that the scattering potential is very small compared to the incident electron energy and that the z component of \vec{k} only varies very slightly during the scattering process. This is a **good approximation** as the mean crystal potential is of the order of 10 - 40 V.
- Electron back scattering is **neglected** (as the z movement is almost constant in the z direction).
- Equation (4) is formally equivalent to a **time-dependent Schrödinger equation** in 2 dimensions $\vec{\rho}$, where z plays the role of time.
- The **evolution** of the system is absolutely **causal**, i.e. from the **past** to the **future** without any interaction towards the past (the -z movement of the electrons does not interfere with the +z movement).

Using a hamiltonian notation equation (4) becomes:

$$i\frac{\partial}{\partial z}\psi = \hat{H}\psi$$
$$\hat{H} = \frac{1}{2k_z} [-\Delta_\rho - \chi^2 + V(\vec{\rho}, z)]$$

Introducing \hat{H}_o as:

$$\hat{H}_o = [-\Delta_\rho + V(\vec{\rho}, z)]$$

\hat{H}_o is the hamiltonian of a system where \vec{k} is parallel to $[u, v, w]$.

$$\hat{H} = \frac{1}{2k_z} [\hat{H}_o - \chi^2]$$

where χ^2 is the **transverse kinetic energy** of the incident electrons (= 0 when the electron beam is along $[u, v, w]$). \hat{H} depends on z through $V(\vec{\rho}, z)$.

When $V = V(\vec{\rho})$ does not depend on z , a **causal evolution operator** $\hat{U}(z, 0)$ is defined as:

$$\psi(\vec{\rho}, z) = \hat{U}(z, 0)\psi(\vec{\rho}, 0)$$

Assuming that V does not depend on z , is equivalent to replace the crystal by a stack of thin slices, with constant potential $V'(\vec{\rho})$ (in a given slice):

$$V'(\vec{\rho}) = \frac{1}{\tau} \int_z^{(z+\tau)} V(\vec{\rho}, z') dz' \quad (5)$$

The causal evolution operator is thus:

$$\hat{U}(z, 0) = \underbrace{\hat{U}(z_n, z_{n-1})}_{\text{slice n}} \underbrace{\hat{U}(z_{n-1}, z_{n-2})}_{\text{slice n-1}} \dots \underbrace{\hat{U}(z_1, 0)}_{\text{slice 1}} \quad (6)$$

The evolution operator obeys the following differential equation (postulate of quantum mechanics)^{3 4}:

$$i\frac{\partial}{\partial z}\hat{U}(z, 0) = \hat{H}(\vec{\rho}, z)\hat{U}(z, 0) \quad (7)$$

Hence, the small angle approximation of the dynamical theory of elastic electron diffraction is solved when $\hat{U}(z, 0)$ is known.

³A. Messiah, *Mécanique Quantique*, Dunod Paris, 1964.

⁴R. Shankar, *Principles of Quantum Mechanics*, Plenum Press, 1994.

Notation

In crystal space, at 2 dimensions, $\vec{\rho} = (x, y)$ or ρ ($\vec{\rho}$ representation), the position eigenvectors are given by:

$$|\rho\rangle = \delta(\vec{\rho}' - \vec{\rho}) \quad (8)$$

In the **dual space** or reciprocal space or momentum space the eigenvectors (plane waves) of the momentum q are given by:

$$|q\rangle = e^{i\vec{q}\cdot\vec{\rho}} \quad (9)$$

In the $\{|\rho\rangle\}$ basis the electron wave-function is:

$$|\psi\rangle = \int \psi(\vec{\rho}') \delta(\vec{\rho}' - \vec{\rho}) d\vec{\rho}' \quad (10)$$

In the $\{|q\rangle\}$ basis the wave-function projected in the \vec{q} direction is:

$$\langle q|\psi\rangle = \int \psi(\vec{\rho}) e^{-i\vec{q}\cdot\vec{\rho}} d\vec{\rho} = \int \psi(\rho) e^{-iq\cdot\rho} d\rho \quad (11)$$

i.e. $\langle q|\psi\rangle$ is the complex amplitude diffracted in the $|q\rangle$ direction. The wave function:

$$\psi(\rho) = \sum_{|q\rangle} \langle q|\psi\rangle$$

is decomposed on a basis of plane waves, i.e. **Fourier decomposition**.

initial state: $|\chi\rangle$

wave function: $\psi(\rho, 0) = \langle \rho|\chi\rangle = \langle \rho|o\rangle$

final state: $|\psi_z\rangle$

wave function: $\psi(\rho, z) = \langle \rho|\psi_z\rangle = \langle \rho|\hat{U}(z, 0)|o\rangle$

Transition probability

Intensity diffracted in $|q\rangle$ direction is transition probability $\omega_{o \rightarrow q}(z, 0)$ from initial state $|o\rangle$ to final state $|q\rangle$:

$$\omega_{o \rightarrow q}(z, 0) = \left| \langle q | \hat{U}(z, 0) | o \rangle \right|^2$$

Intensity at point $\vec{\rho}$ of crystal exit plane:

$$\omega_{o \rightarrow \rho}(z, 0) = \left| \langle \rho | \hat{U}(z, 0) | o \rangle \right|^2 = \left| \sum_q \langle \rho | q \rangle \langle q | \hat{U}(z, 0) | o \rangle \right|^2$$

Closure for periodic specimen: $\sum_q |q\rangle \langle q| = \hat{I}$.

Intensity observed at point $\vec{\rho}$ located in image plane (observation plane) is modified by microscope transfer function $\hat{T}(q', q)$:

$$\omega_{o \rightarrow \rho}(z, 0) = \left| \sum_{q'} \sum_q \langle \rho | q' \rangle \langle q' | \hat{T}(q', q) | q \rangle \langle q | \hat{U}(z, 0) | o \rangle \right|^2$$

This was the mysterious formula of the image formation in TEM!

When the transfer is linear (i.e. for a weak phase object), the transfer matrix is diagonal $\langle q' | \hat{T}(q', q) | q \rangle = \hat{T}(q) \delta(q' - q)$. Then:

$$\omega_{o \rightarrow \rho}(z, 0) = \left| \sum_q' \sum_q \langle \rho | q' \rangle T(q) \langle q | \hat{U}(z, 0) | o \rangle \right|^2$$

Last step is calculation of evolution operator $\hat{U}(z, 0)$. $\hat{U}(z, 0)$, a unitary operator, is not generally integrable.

But when:

- $V(\vec{\rho}, z)$ does not depend on z (Bloch-wave method)
- or $V(\vec{\rho}, z)$ can be neglected (Fresnel propagator)
- or $\hat{H}(\vec{\rho}, z)$ reduces to its potential term (Phase Grating),

$\hat{H}(\rho, z)$ and $\frac{\partial}{\partial z} \hat{H}(\rho, z)$ commute and $\hat{U}(z, 0)$ is directly integrable.

Hermitic or self-adjoint operator

Hermitic or self-adjoint operators can be decomposed on the basis formed by their eigenvectors (**spectral decomposition**). For example:

$$\hat{H} = \sum_i \lambda_i |\lambda_i\rangle \langle \lambda_i| \quad (12)$$

$$= \sum_i \lambda_i \hat{P}_{\lambda_i} \quad (13)$$

where λ_i is the eigenvalue and $|\lambda_i\rangle$ the eigenvector and $\hat{P}_{\lambda_i} = |\lambda_i\rangle \langle \lambda_i|$ are projection operators.

Using spectral decomposition, any function of a hermitic operator, $f(\hat{H})$, can be written as:

$$f(\hat{H}) = \sum_i f(\lambda_i) |\lambda_i\rangle \langle \lambda_i|$$
$$= \sum_i f(\lambda_i) \hat{P}_{\lambda_i}$$

since $\hat{P}_{\lambda_i}^n = \hat{P}_{\lambda_i}$ (any function can be developed in a Taylor series).

Bloch wave method

Scattering potential **does not depend on z**, it is evaluated by projecting the unit cell potential on a plane perpendicular to $[u, v, w]$ zone axis (only **Zero Order Laue Zone** reflections (hkl), i.e. $hu + kv + lw = 0$).

$$\hat{U}(z, 0) = e^{-[i \int_0^z \hat{H}(\rho) d\tau]} = e^{-i\hat{H}(\rho)z}$$

Since \hat{H} is a self-adjoint (hermitic) operator, it can be represented in its eigenstates basis $\{|\alpha\rangle\}$ by a diagonal matrix $\hat{\gamma}_\alpha$ where the γ_α are the associated eigenvalues:

$$\hat{H}|\alpha\rangle = \hat{\gamma}_\alpha|\alpha\rangle$$

The eigenstates are **Bloch waves** that characterise the propagation of the incident electron wave in a periodic continuum (crystal) and the eigenvalues γ_α give the **kinetic energy** of the Bloch waves. The unitary operators $\hat{P}_\alpha = |\alpha\rangle\langle\alpha|$ are the projectors on the eigenstates of $\hat{H}(\rho)$.

$$\hat{H} = \sum_{\alpha} \gamma_{\alpha} |\alpha\rangle\langle\alpha| = \sum_{\alpha} \gamma_{\alpha} \hat{P}_{\alpha}$$

Finally:

$$\hat{U}(z, 0) = \sum_{\alpha} e^{-i\gamma_{\alpha}z} |\alpha\rangle\langle\alpha| \quad (14)$$

The incident wave function $|o\rangle$ is a plane wave (or a sum of plane waves). Using the principle of superposition, it suffices to consider only one plane wave to calculate the wave function $\psi(\rho, z)$ at the exit plane of the crystal:

$$\psi(\rho, z) = \sum_q \phi_q(\rho, z) |q\rangle$$

With:

$$|\psi_z\rangle = \sum_\alpha e^{-i\gamma_\alpha z} |\alpha\rangle \langle \alpha | \psi_o \rangle$$

$\phi_q(\rho, z)$ (Fourier coefficient of the wave transmitted by the crystal, i.e. reflection in \vec{q} direction ($\vec{q} = \vec{g} + \vec{s}_g$)) is:

$$\phi_q(\rho, z) = \langle q | \psi_z \rangle = \langle q | \hat{U}(z, 0) | o \rangle = \sum_\alpha e^{-i\gamma_\alpha z} \langle q | \alpha \rangle \langle \alpha | o \rangle \quad (15)$$

Many books and research papers use Bloch wave "excitation" and "coefficients". They are expressed in basis $|q\rangle$ and $|\alpha\rangle$ as:

- $\langle \alpha | o \rangle = (c_o^\alpha)^* = c_o^{\alpha*}$ projection of $|o\rangle$ on $|\alpha\rangle$: **excitation coefficients**.
- $\langle q | \alpha \rangle = c_q^\alpha$ projection of $|\alpha\rangle$ on $|q\rangle$: **Bloch wave coefficients**.

$$\psi(\rho, z) = \langle q | \hat{U}(z, 0) | o \rangle = \sum_\alpha c_o^{\alpha*} e^{-i\gamma_\alpha z} \sum_q c_q^\alpha |q\rangle \quad (16)$$

The Bloch waves (eigenstates) are linear combinations of plane waves:

$$|\alpha\rangle = \sum_q c_q^\alpha |q\rangle$$

Bloch wave example: ZnTe [110]

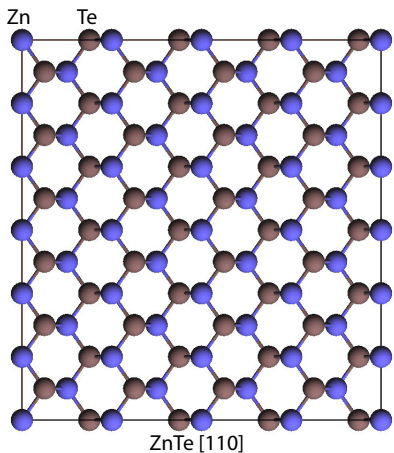


Figure: ZnTe [110].

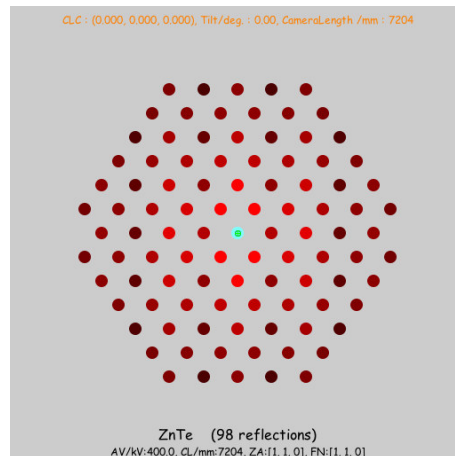


Figure: Reflections (1 + 49), $|\chi| \geq 0$.

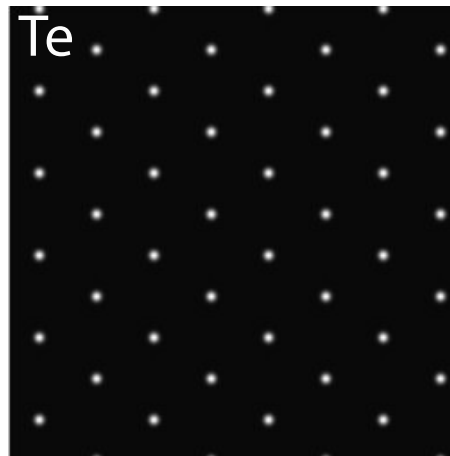


Figure: Bloch-wave 1 (Te 1s).

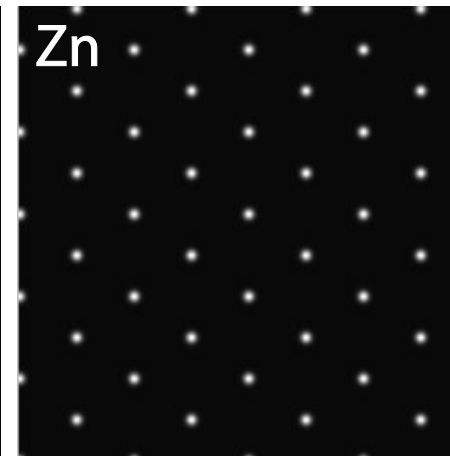


Figure: Bloch-wave 2 (Zn 1s).

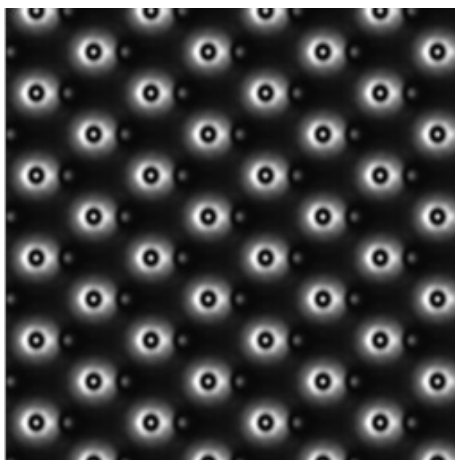


Figure: Bloch-wave 5 (Te-Zn).

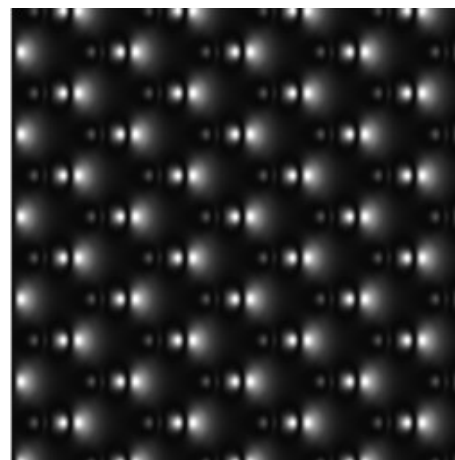


Figure: Bloch-wave 7 (Te-Zn).

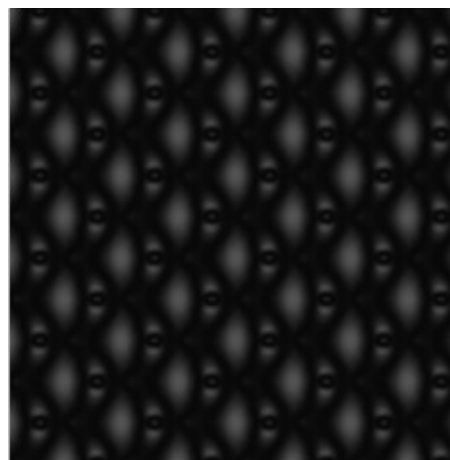


Figure: Bloch-wave 8 (Te-Zn).

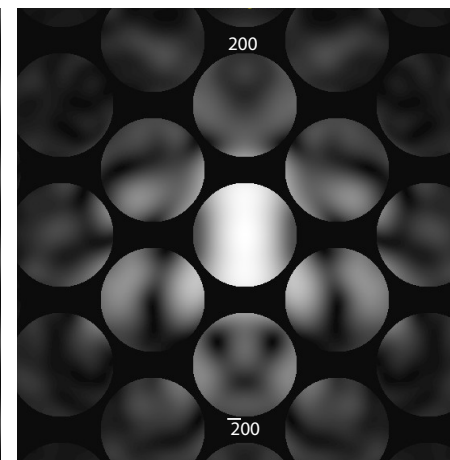


Figure: CBED (ZnTe polarity).

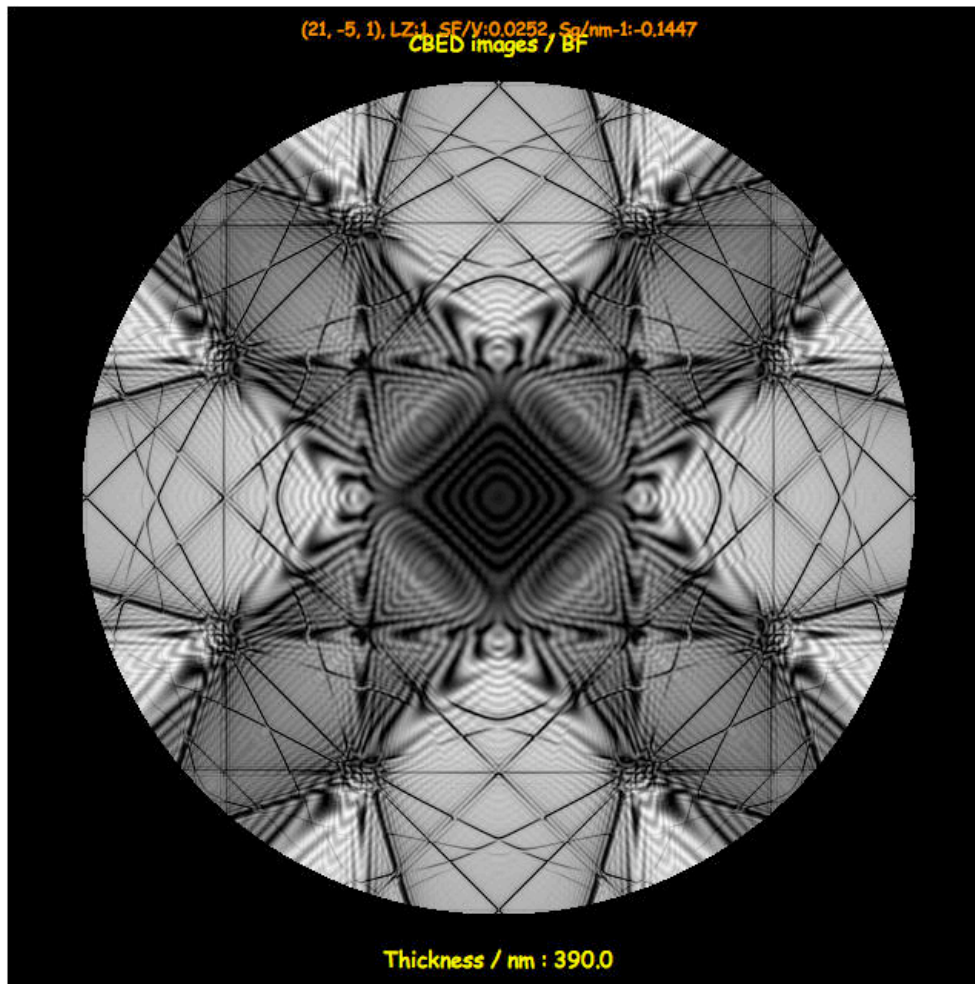


Figure: LACBED Si [001]: simulation.

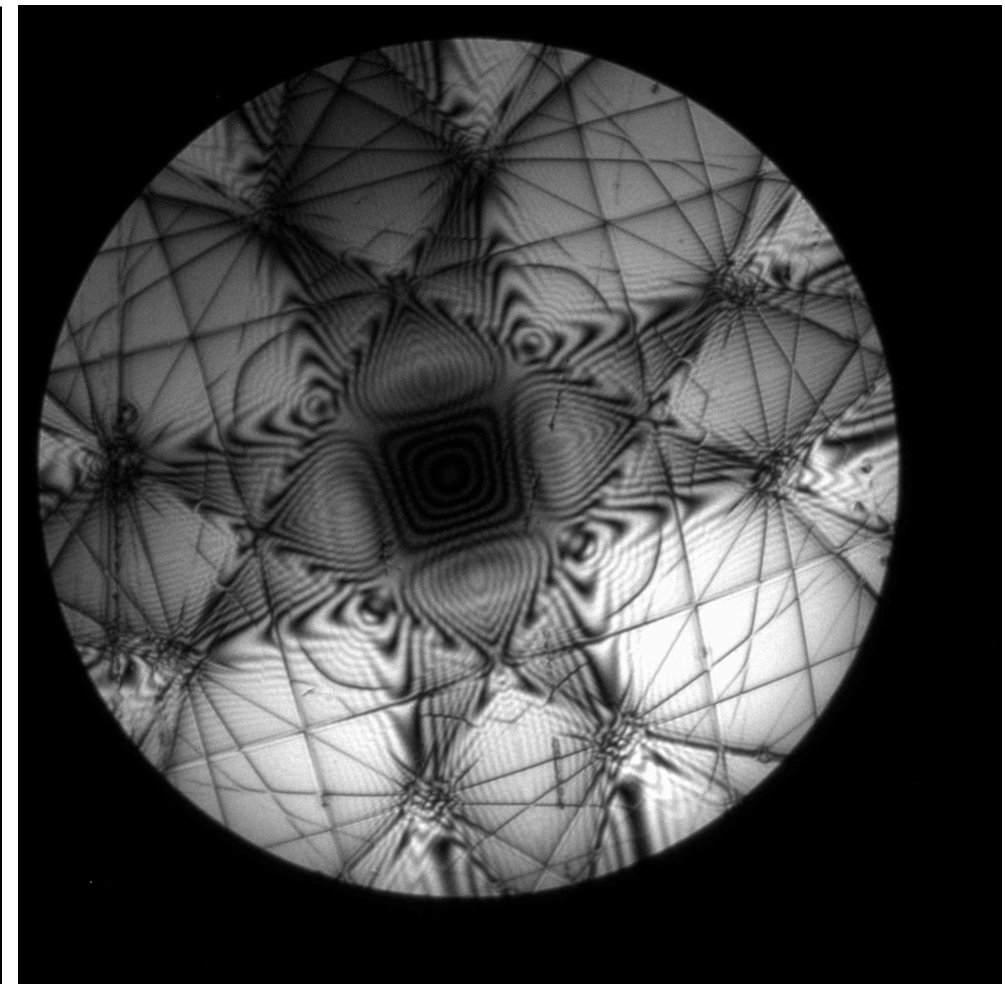


Figure: LACBED Si [001]: experimental (Web site EM centre - Monash university, J. Etheridge).

⁵file://localhost/Applications/jemsMacOSX/html/Si001/Si001.html

This method consist to transfer the incident wave function through a plane, acting as a phase grating, and to propagate the transmitted wave to the next slice. 2 operators (matrices) must be calculated:

- Phase object (Phase Object Function).
- Propagator (Fresnel approximation).

Phase Object Function

\hat{H} reduces to $\frac{1}{2k_z}\hat{V}(\vec{\rho}, z)$. \hat{H} is diagonal in the $|\rho\rangle$ representation.

$$\hat{H}(z)|\rho\rangle = \frac{1}{2k_z}\hat{V}(\vec{\rho}, z)|\rho\rangle$$

The evolution operator is:

$$\hat{U}(z, 0) = \int_{\rho} d\rho |\rho\rangle \langle \rho| e^{[\frac{-i}{2k_z} \int_0^z V(\vec{\rho}, \tau) d\tau]} \quad (17)$$

At thickness z the wave function is: and $|\psi_z\rangle = \hat{U}(z, 0)|o\rangle = e^{-i\frac{1}{2k_z}V_p(\vec{\rho})}|o\rangle$ ($\frac{1}{2k_z}$ is very small compared to $V_p(\vec{\rho})$).

Phase Object Function:

$$POF(\vec{\rho}) = e^{-i\frac{1}{2k_z}V_p(\vec{\rho})}$$

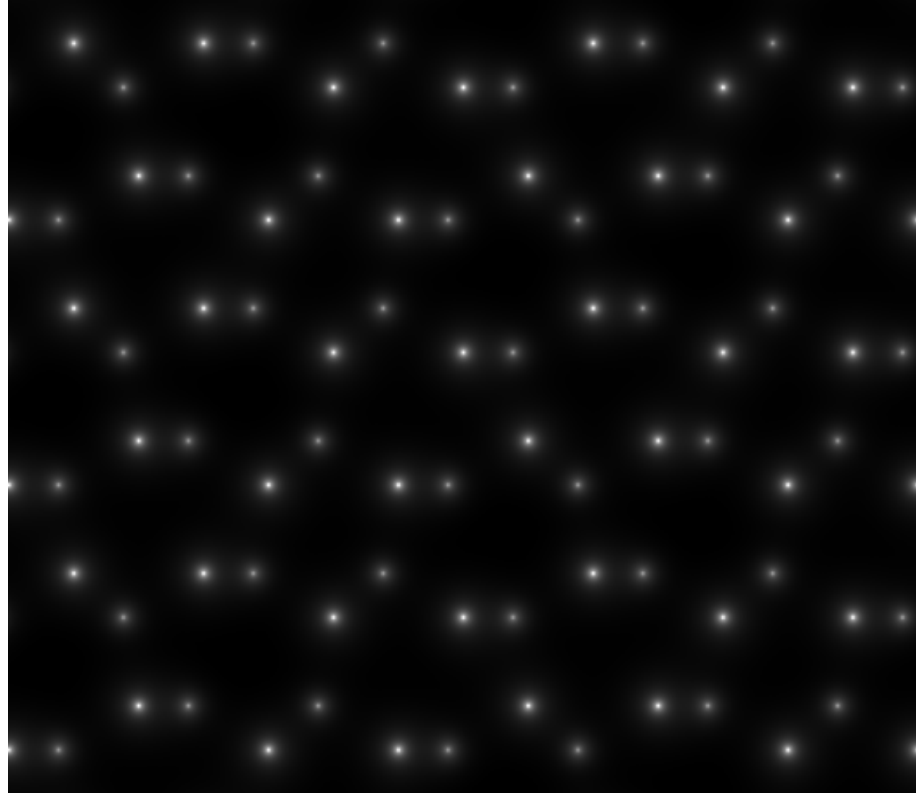
The Weak Phase Object approximation uses a first order Taylor approximation of the phase object function:

$$POF(\vec{\rho}) = 1 - i\frac{1}{2k_z}V_p(\vec{\rho}) = 1 + i\sigma \int_0^z V_v(\vec{\rho}, \tau) d\tau \quad (18)$$

$POF(\vec{\rho})$: Phase Object Function



$POF(\vec{\rho})$ (real part).



$POF(\vec{\rho})$ (imaginary part).

This approximation describes the propagation of the electron wave in vacuum.

$$\hat{H} = \frac{1}{2k_z} [-\Delta_\rho - \chi^2]$$

\hat{H} is diagonal in the $\{|q\rangle\}$ basis.

$$\hat{H}|q\rangle = \frac{q^2 - \chi^2}{2k_z}|q\rangle$$

The evolution operator is also diagonal in $\{|q\rangle\}$:

$$\hat{U}(z, 0) = \sum_q e^{-i\frac{q^2 - \chi^2}{2k_z}z} |q\rangle \langle q|$$

Without a scattering potential, the incident wave function intensity is not modified:

$$\left| \hat{U}(z, 0) |o\rangle \right|^2 = ||o\rangle|^2$$

In real space propagation from point $\vec{\rho}_1$ to point $\vec{\rho}_2$ (on 2 planes separated by a distance z) is given by:

$$\langle \rho_2 | \hat{U}(z, 0) | \rho_1 \rangle = \int_q e^{-i \frac{q^2 - \chi^2}{2k_z} z} \langle \rho_2 | q \rangle \langle q | \rho_1 \rangle \quad (19)$$

Since:

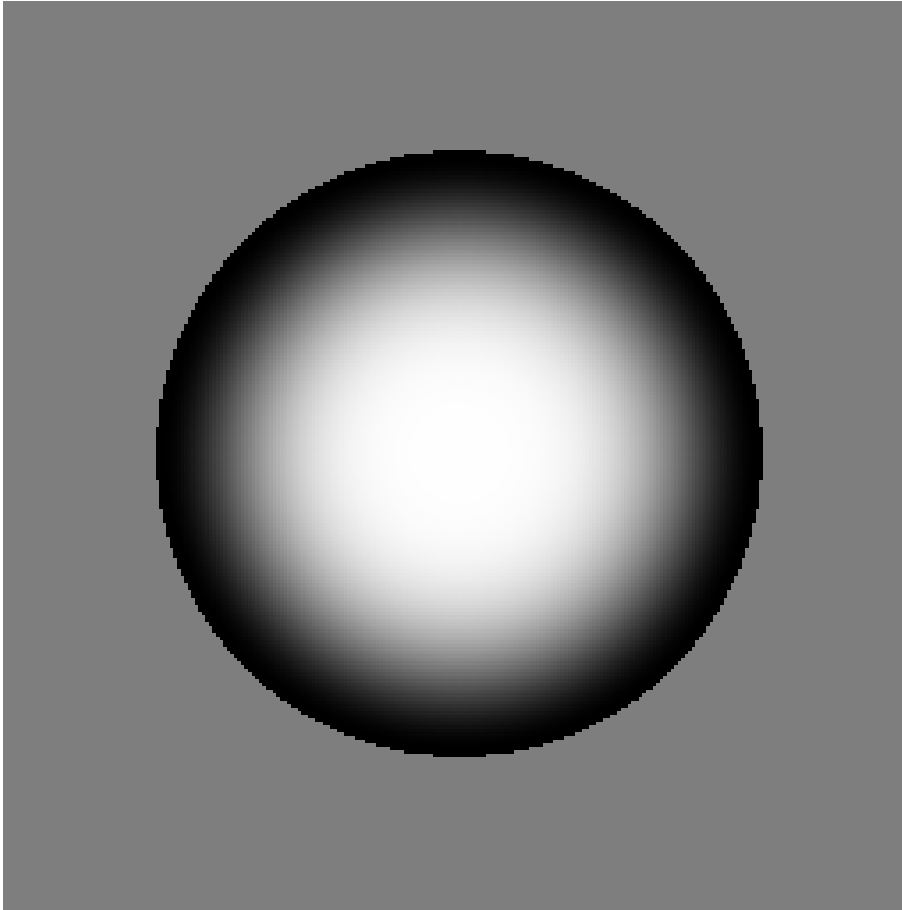
$$\langle \rho_2 | q \rangle = \int d\vec{q} \delta(\vec{\rho} - \vec{\rho}_2) e^{i\vec{q} \cdot \vec{\rho}}$$

$$\langle q | \rho_1 \rangle = \int d\vec{q} \delta(\vec{\rho} - \vec{\rho}_1) e^{-i\vec{q} \cdot \vec{\rho}}$$

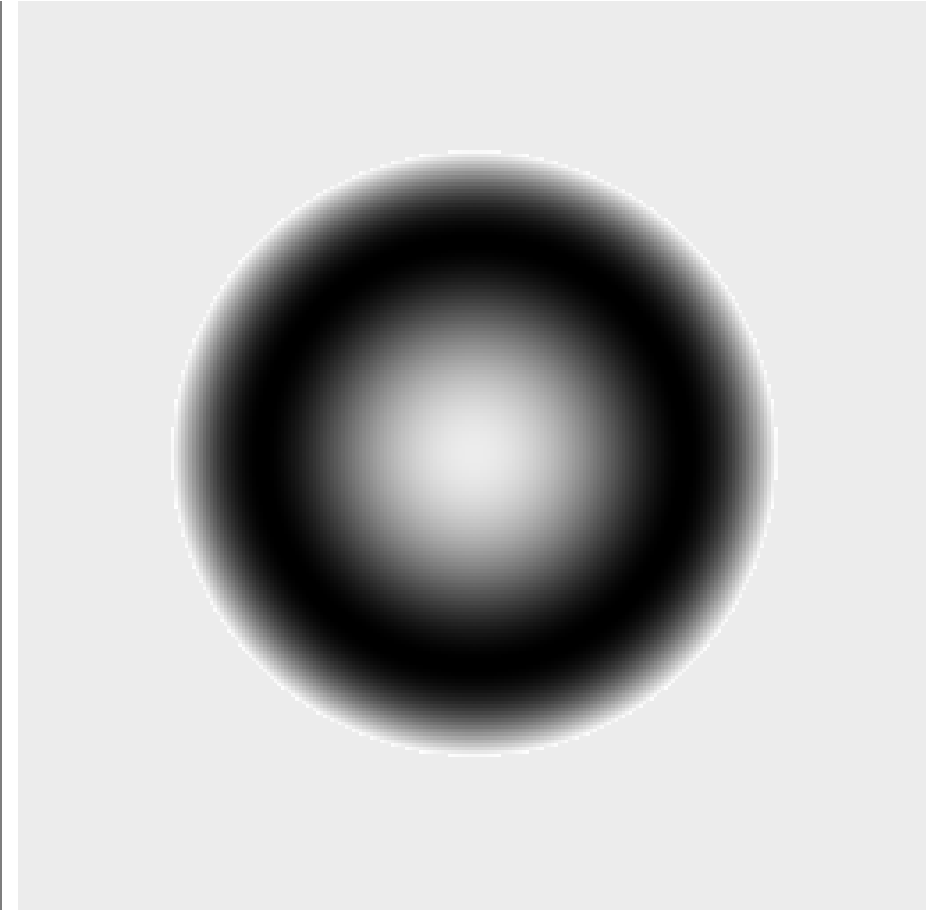
Finally when $\chi = 0$:

$$\langle \rho_2 | \hat{U}(z, 0) | \rho_1 \rangle = \int d\vec{q} e^{-i \frac{q^2}{2k_z} z} e^{-i\vec{q} \cdot (\vec{\rho}_1 - \vec{\rho}_2)}$$

$$FP(\vec{\rho}_1 - \vec{\rho}_1) = e^{\frac{-ik_z(\vec{\rho}_1 - \vec{\rho}_2)^2}{z}}$$



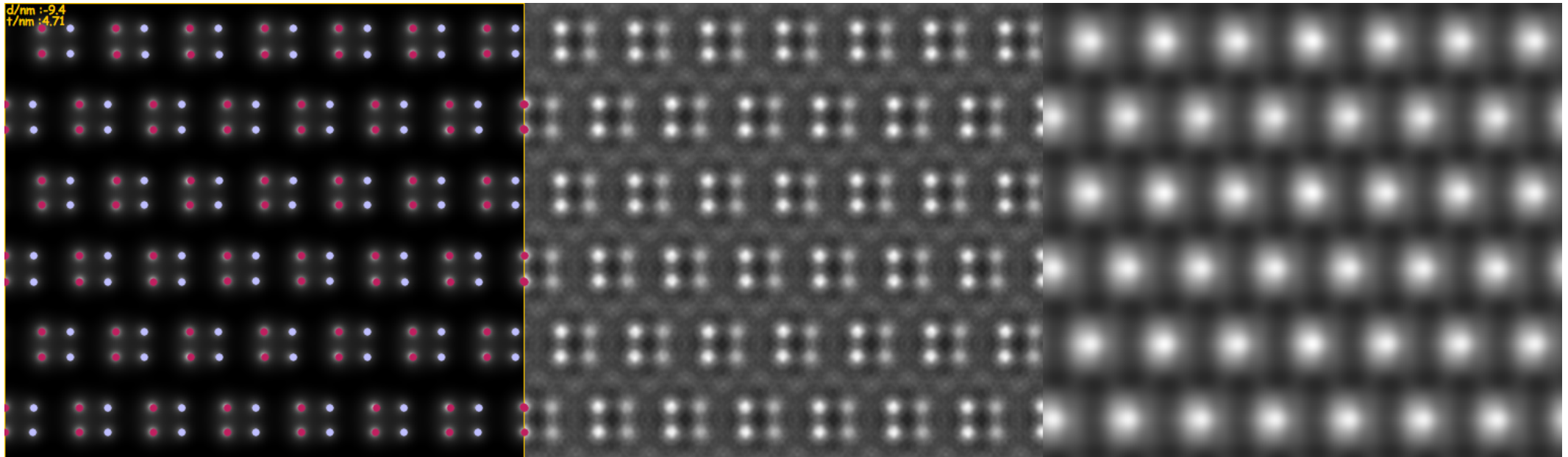
$\widetilde{FP}(u, v)$ (real part).



$\widetilde{FP}(u, v)$ (imaginary part).

Wave function after slice $n + 1$ ($\vec{\rho} = (x, y)$):

$$\Psi_{n+1}(\vec{\rho}) = [\Psi_n(\vec{\rho}) \otimes FP(\vec{\rho})] POF(\vec{\rho})$$



AlN [1,1,1] (4.71 nm thick) (projected potential + atoms position, wave-function, image)

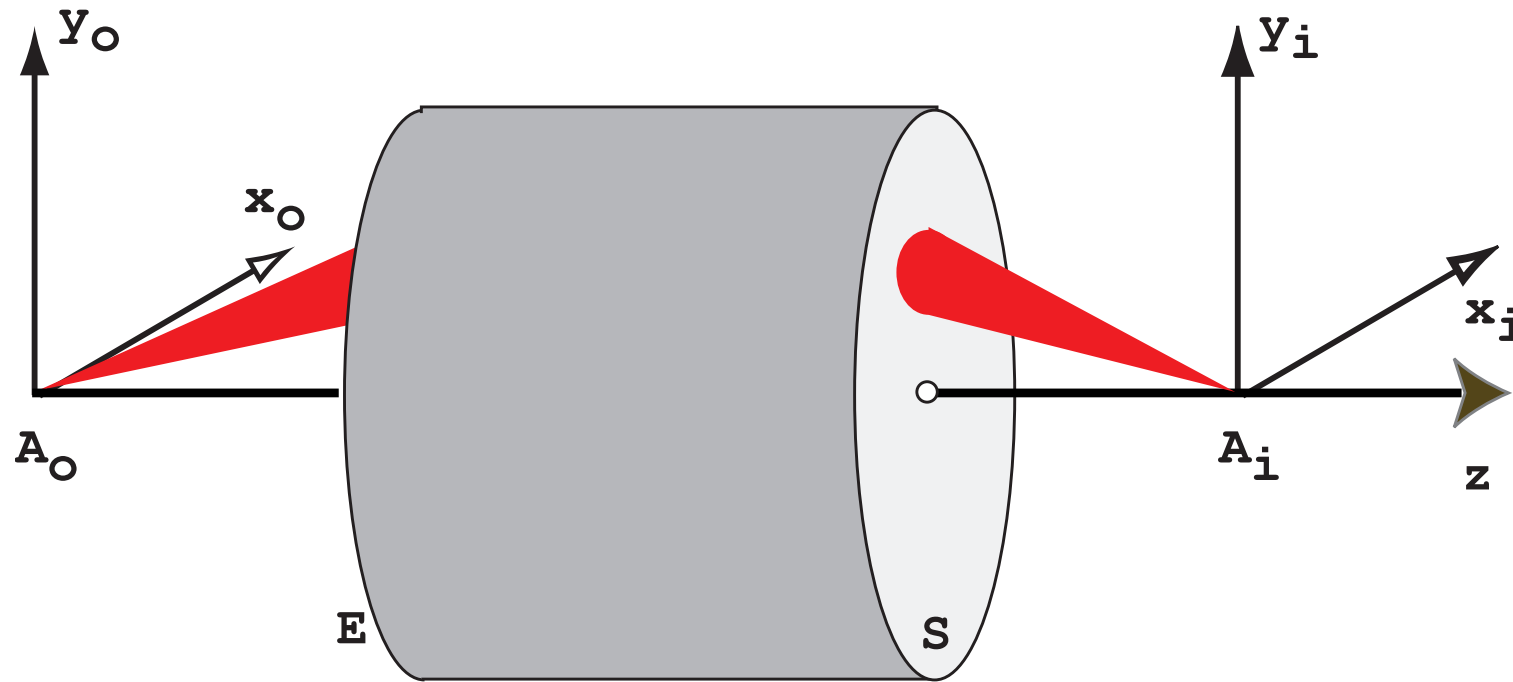
Wave-function after slice $n + 1$:

$$\Psi_{n+1}(x, y) = [\Psi_n(x, y) \otimes FP(x, y)] POF_{n+1}(x, y)$$

or:

$$\Psi_{n+1}(\vec{x}) = [\Psi_n(\vec{x}) \otimes FP(\vec{x})] POF_{n+1}(\vec{x})$$

- Dynamical scattering.
- —→ **Optical system.**
- Comparing HRTEM and HRSTEM.



An optical system produces the **image** A_i of a **point source** object A_o . A_o and A_i are said to be conjugate. A_i is **not** a point but spot, the Airy disk, since **any optical system is diffraction limited**. This limitation is introduced by the entrance and exit pupils of the optical system. Its point spread function characterise the system:

$$PSF(\vec{\rho}) = FT^{-1} [T(\vec{q})]$$

Linearity

$$\begin{aligned} S\{a_1\Psi_o^1(\vec{x}) + a_2\Psi_o^2(\vec{x})\} &= a_1S\{\Psi_o^1(\vec{x})\} + a_2S\{\Psi_o^2(\vec{x})\} \\ S\{a_1\Psi_o^1(\vec{x}) + a_2\Psi_o^2(\vec{x})\} &= a_1\Psi_i^1(\vec{x}) + a_2\Psi_i^2(\vec{x}) \end{aligned}$$

Linearity allows to decompose the object wave-function in ∞ sum of point sources:

$$\Psi_o(\vec{x}) = \int_{-\infty}^{\infty} \Psi_o(\vec{\zeta})\delta(\vec{x} - \vec{\zeta})d\vec{\zeta}$$

Image wave-function $\Psi_i(\vec{x})$:

$$\Psi_i(\vec{x}) = S\left\{\int_{-\infty}^{\infty} \Psi_o(\vec{\zeta})\delta(\vec{x} - \vec{\zeta})d\vec{\zeta}\right\} = \int_{-\infty}^{\infty} \Psi_o(\vec{\zeta})S\{\delta(\vec{x} - \vec{\zeta})\}d\vec{\zeta}$$

$$\Psi_i(\vec{x}) = \int_{-\infty}^{\infty} \Psi_o(\vec{\zeta})T(\vec{x}; \vec{\zeta})d\vec{\zeta}$$

where $T(\vec{x}; \vec{\zeta}) = S\{\delta(\vec{x} - \vec{\zeta})\}$: **Impulse Response** of optical system S.

Space invariance

Space invariance is realised when the image of a point source is independent of its position in the object plane, i.e. when the point source moves in the object plane its image moves similarly in the image plane without changing form and intensity.

$$T(\vec{x}; \vec{\zeta}) = T(\vec{x} - \vec{\zeta})$$

$$\Psi_i(\vec{x}) = \int_{-\infty}^{\infty} \Psi_o(\vec{\zeta}) T(\vec{x} - \vec{\zeta}) d\vec{\zeta} = \Psi_o(\vec{x}) \otimes T(\vec{x})$$

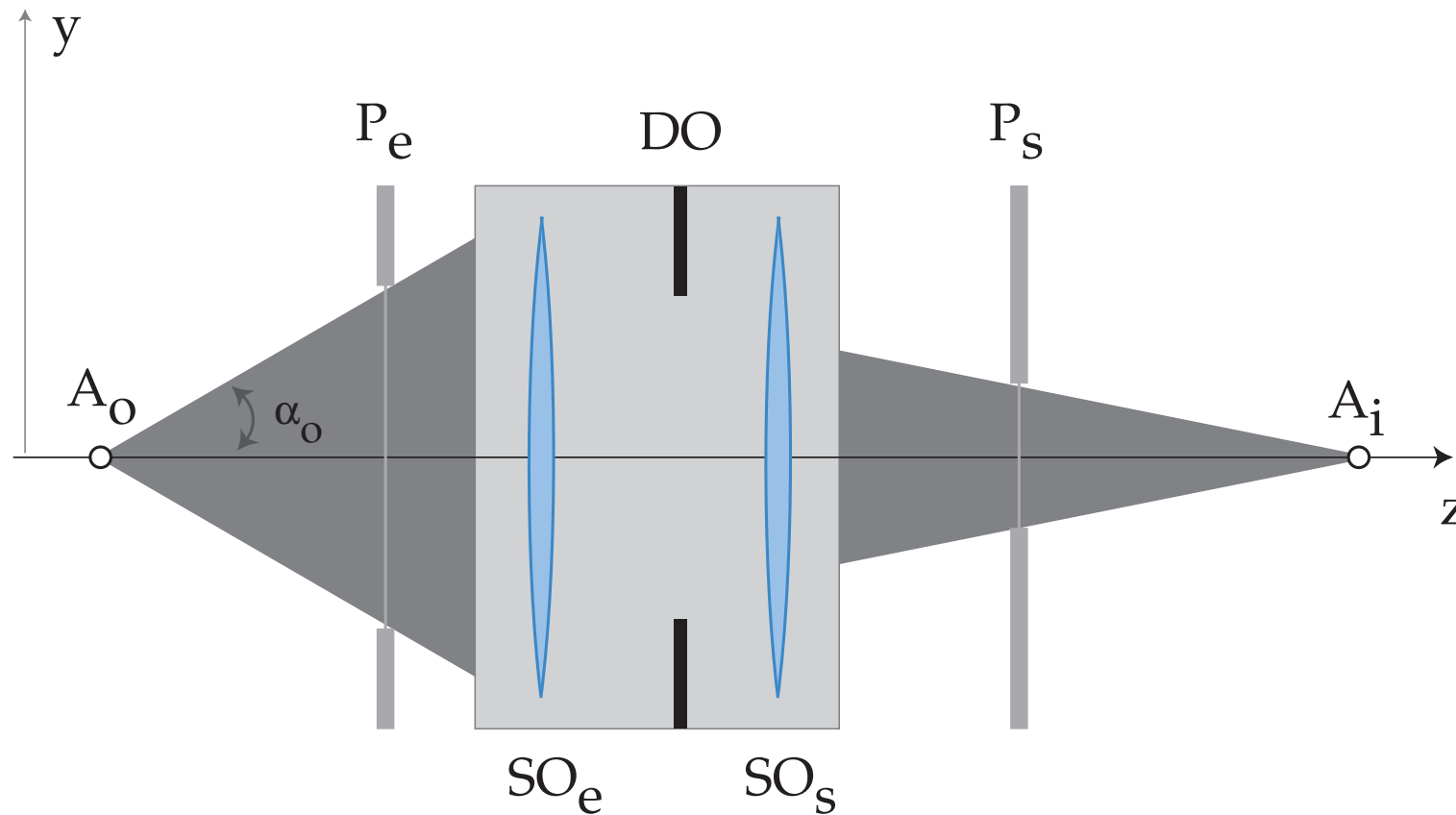
Convolution integral spreads object information, degrades performance of optical system.

In Fourier space:

$$\tilde{\Psi}_i(\vec{q}) = \tilde{\Psi}_o(\vec{q}) \tilde{T}(\vec{q})$$

$\tilde{T}(\vec{q})$: **transfer function** of optical system.

Pupils

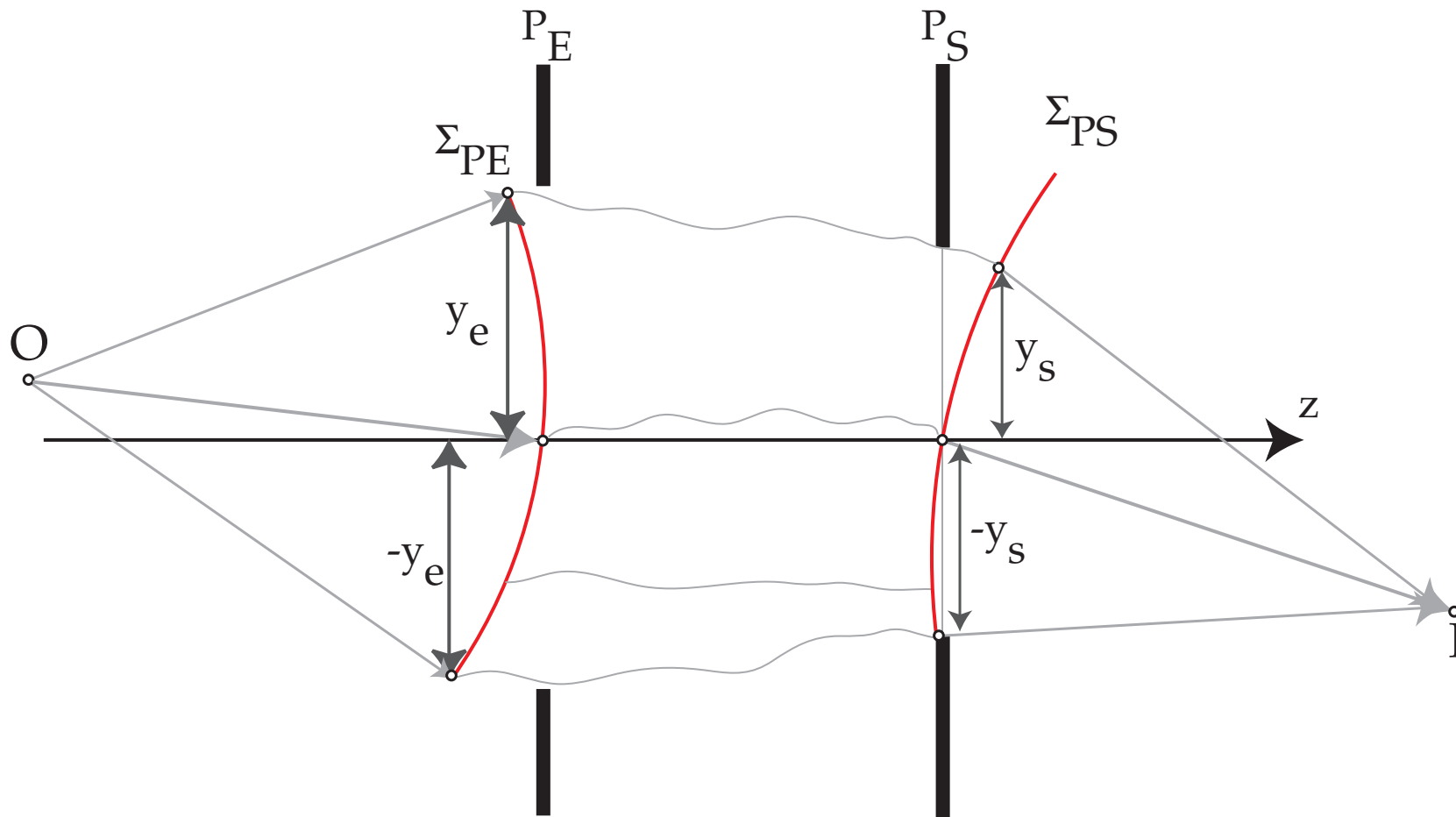


Any optical system can be characterised by an **entrance pupil** P_e and an **exit pupil** P_s . The pupils are the image of the opening aperture DO by the entrance and exit optical sub-systems SO_e and SO_s . The portion of the object wave-function accepted by the optical system is limited by P_e , while SO_s limits the extend of the image wave-function. For a **perfect** optical system, the image of a point source will be an **Airy disk** since only a portion of the incident spherical wave is transferred.

The important feature is the optical path length (OPL).

$$OPL(P_1P_2) = \int_{P_1}^{P_2} n(\vec{r}) ds$$

- 1 OPL is measured in meters ($n(\vec{r}) = \frac{c}{v(\vec{r})}$ has no unit).
- 2 OPL is proportional to the time spent by the light ray to travel from P_1 to P_2 .
- 3 Surface of constant OPL \longrightarrow wavefront (surface of constant travel time).
- 4 OPL is measured from the entrance pupil P_E to the exit pupil P_S .



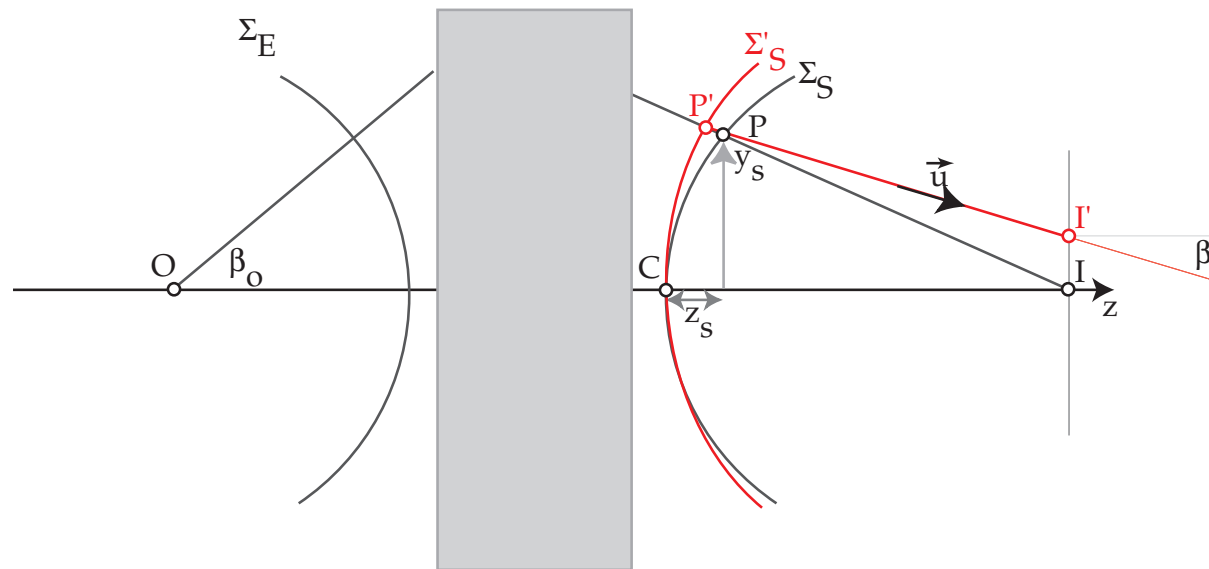
- **Before** P_E the reference wavefront Σ_{PE} is spherical (point source at O).
- **After** P_S the reference wavefront Σ_{PS} is spherical (converges towards I).

For a perfect optical system, both the entrance Σ_{PE} and exit Σ_{PS} wavefronts are spherical. The **Optical Path Length** from O to I is independent of the path.

Optical Path Difference: OPD

The OPD measure the deviation of a wavefront from a perfect spherical wavefront (vacuum or homogenous medium).

At the exit pupil P_S , the spherical wavefront converging towards I defines the reference wavefront.



In the presence of aberrations the wavefront Σ'_S is no more spherical. The **Optical Path Difference**, $\overline{P'P}$ (distance between the deformed Σ'_S and spherical wavefront Σ_S) introduces the **phase shift $\delta\phi$** :

$$\delta\phi = e^{2\pi i \frac{OPD(x_S, y_S)}{\lambda}}$$

Transfer function $\tilde{T}(\vec{q})$

The summation of the phase shifts $\delta\phi$ make up the transfer function $\tilde{T}(\vec{q})$.

$$\tilde{T}(\vec{q}) = e^{-i\chi(\vec{q})} = \cos(\chi(\vec{q})) - i \underbrace{\sin(\chi(\vec{q}))}_{\text{PCTF}}$$

Phase Contrast Transfer Function:

$$\chi(\vec{q}) = \pi \left[-W_{20} \lambda (\vec{q} \cdot \vec{q}) + W_{40} \frac{\lambda^3 (\vec{q} \cdot \vec{q})^2}{2} + \dots \right]$$

Where:

- W_{20} : defocus (z)
- W_{40} : spherical aberration (C_s)

At present TEM and STEM aberration correctors only correct axial aberrations, i.e. aberrations that affect images of point sources located on the optical axis.

Aberrations: how to define them

Some light rays emitted by object point A_o do not reach the image at point A_i .

Position of A_i \longrightarrow intersection of the reference light ray (non deviated) and the image plane.

The image of a point source is a **spot** whose shape and intensity depend of the quality of the optical system.

Two types of aberrations:

- 1 **Monochromatic.**
- 2 Chromatic (λ dependent).

In order to evaluate the monochromatic aberrations one must define a function characteristic of the optical system.

This function will depend on:

- 1 The selected reference planes.
- 2 The optical path followed by the light ray.

Transverse geometric aberrations: $\vec{\epsilon}$

The transverse geometric aberrations are proportional to $\frac{d}{d\theta}$ wavefront aberrations⁶:

$$\epsilon_x = -\frac{f \partial W}{n_i \partial x_s}$$
$$\epsilon_y = -\frac{f \partial W}{n_i \partial y_s}$$

f focal length.

The OPD's introduced by all the aberrations of the imaging system are collected in a function $\chi(\vec{q})$ and the phase shift is⁷:

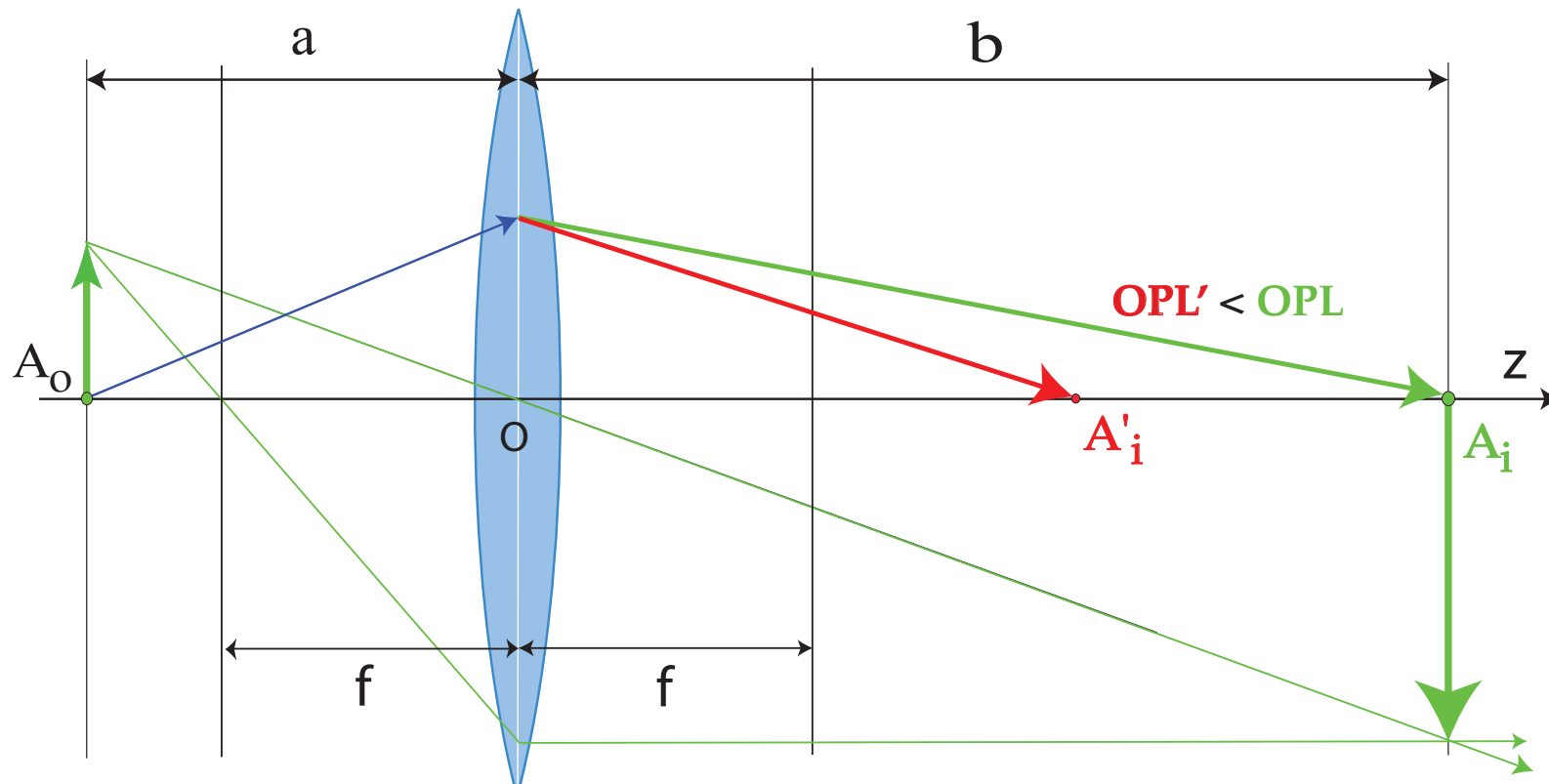
$$\tilde{T}(\vec{q}) = e^{-i\chi(\vec{q})}$$

$\tilde{T}(\vec{q})$ has been first employed by Abbe in his description of image formation (1866).

⁶ $P(x_s, y_s)$ on the spherical reference wavefront can be characterised by the radial angle θ .

⁷The angle θ corresponds (through Bragg law) to a spatial frequency \vec{q} , i.e. a distance in the back focal plane.

OPD: spherical aberration

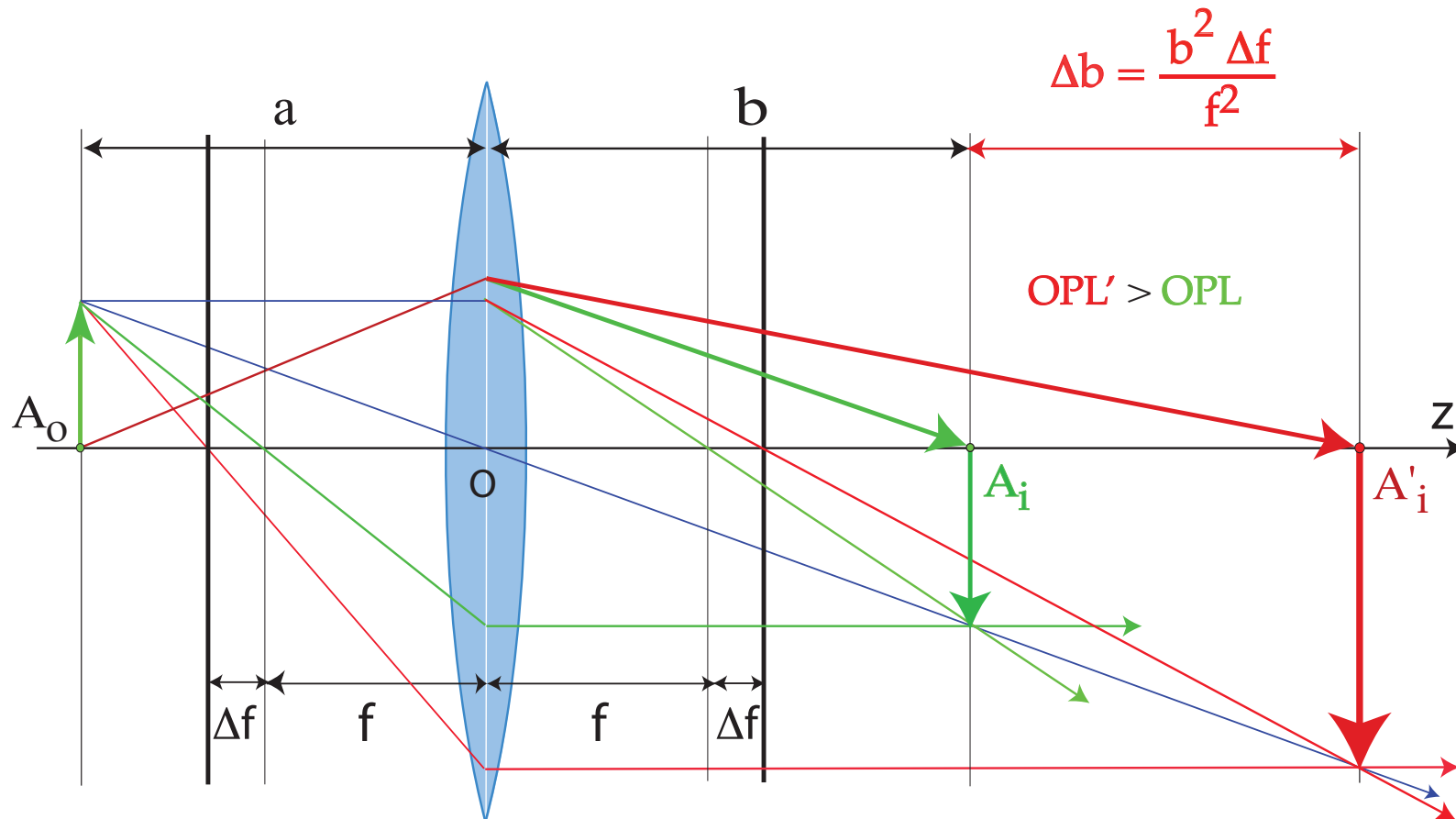


In presence of spherical aberration, the optical path length (OPL') from A_o to A'_i is smaller than OPL from A_o to A_i . The wavefront at A'_i is out-of-phase by⁸:

$$e^{-2\pi i \frac{C_s \lambda^3 (\vec{q} \cdot \vec{q})^2}{4}}$$

⁸With our plane wave choice $e^{2\pi i \vec{q} \cdot \vec{r}}$.

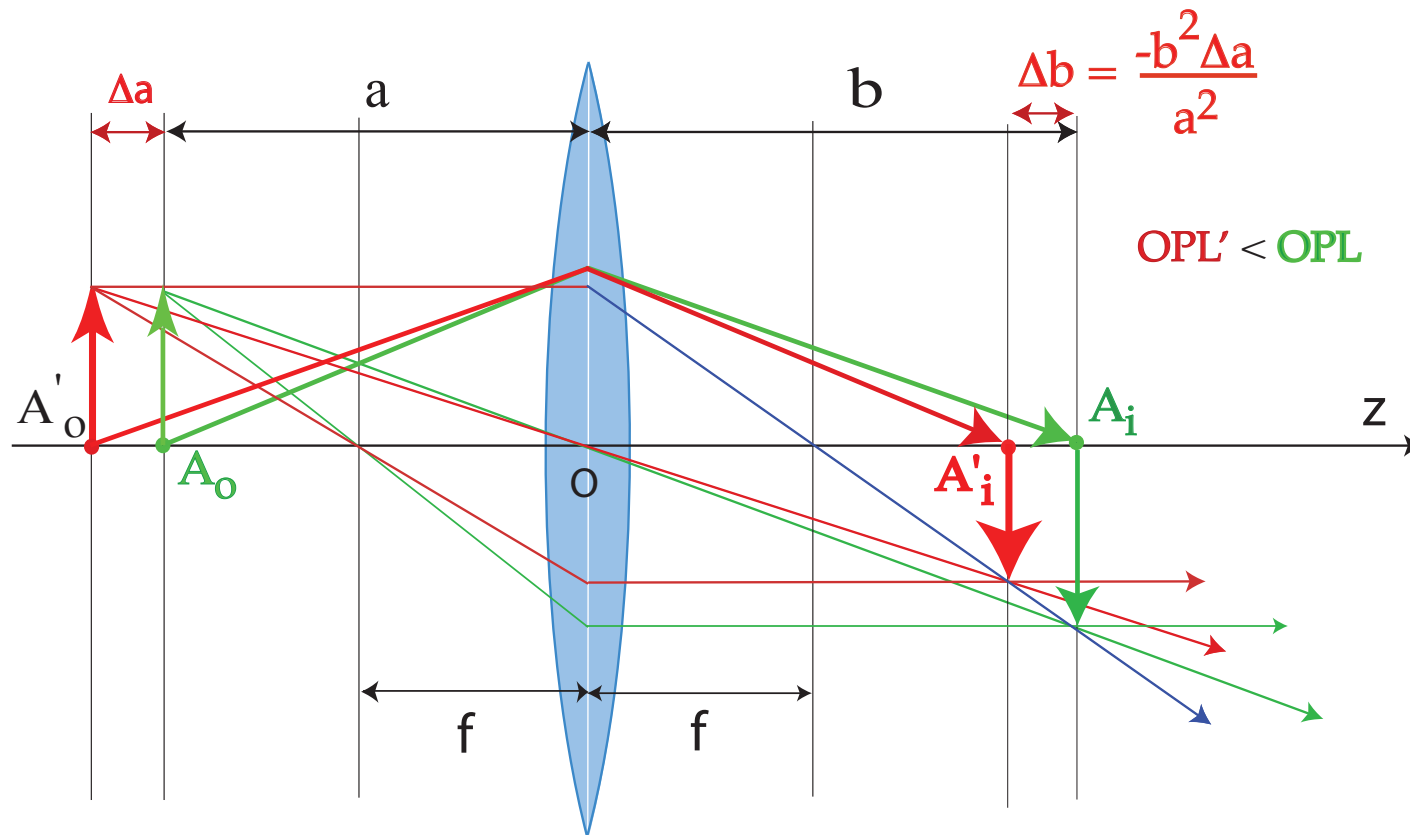
OPD: underfocus



Underfocus weakens the objective lens, i.e. increases f . As a consequence the OPL from A_o to A'_i is larger:

$$e^{2\pi i \frac{\Delta f \lambda (\vec{q} \cdot \vec{q})}{2}}$$

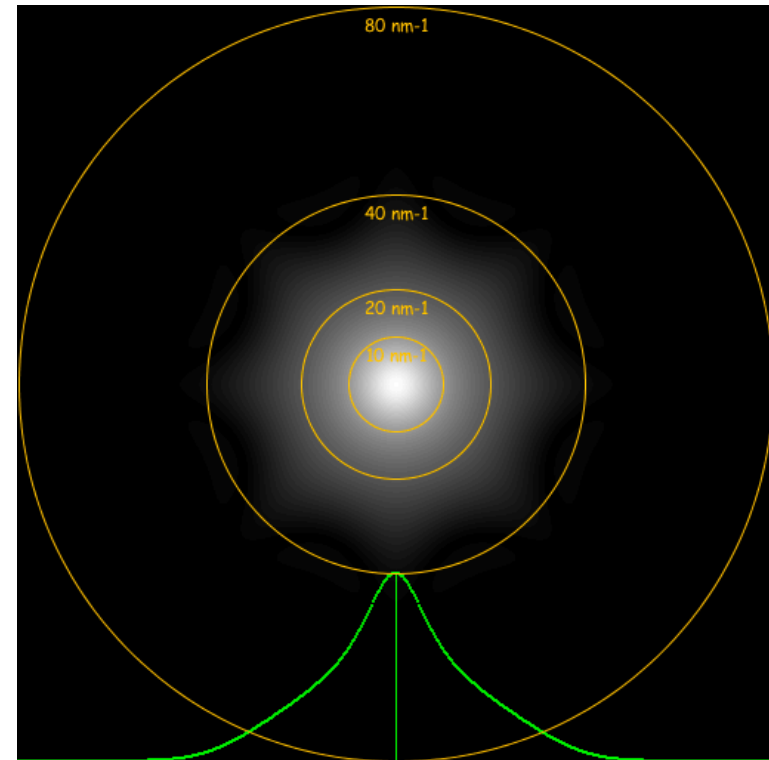
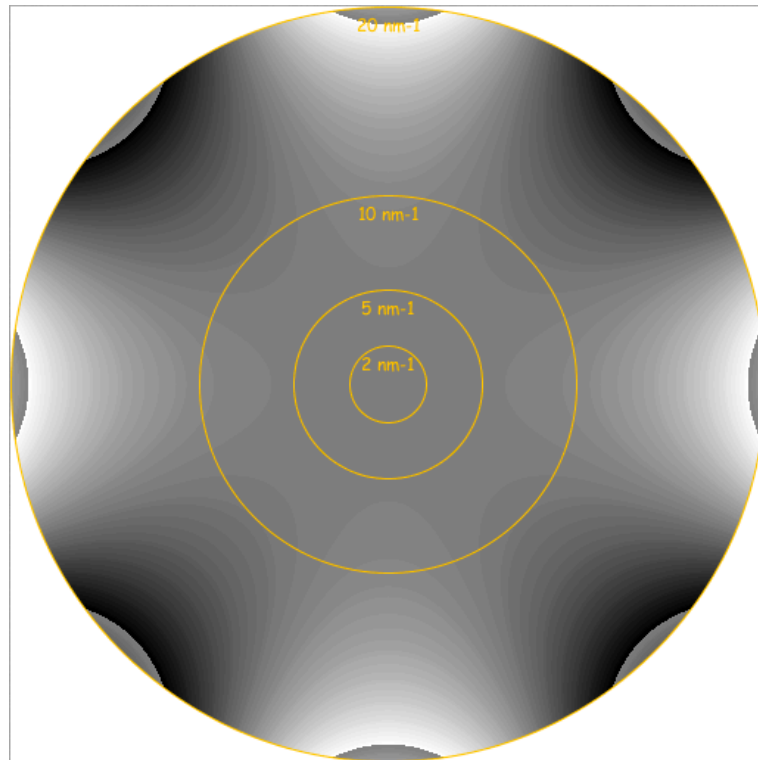
OPD: eccentricity



On the contrary keeping f constant and moving the object by Δa decreases the OPL.

HRTEM / HRSTEM problem: aberrations of optical system

Reaching 0.05 nm resolution sets very strong conditions on aberrations correction.



Aberration figure of $C_{34}(0.5\mu\text{m})$, phase jump at $\frac{\pi}{4}$.

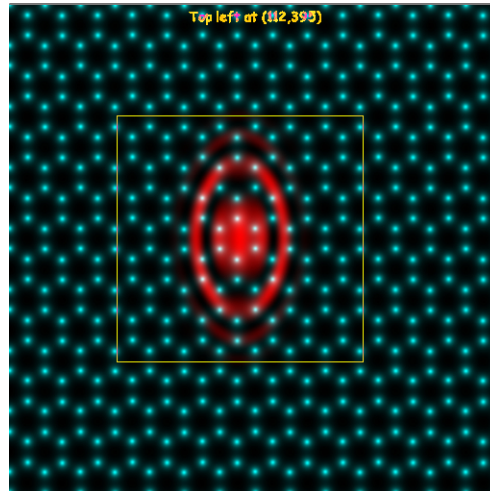
Optical Transfer Function.

Notice that **Optical Transfer Function** (HRSTEM) transfers **higher spatial frequencies** than **Coherent Transfer Function** (HRTEM). OTF is the autocorrelation of the PSF with itself. Autocorrelation **doubles** the domain of the function \longrightarrow the $OTF(\vec{q})$ domain is twice as large as the $TF(\vec{q})$.

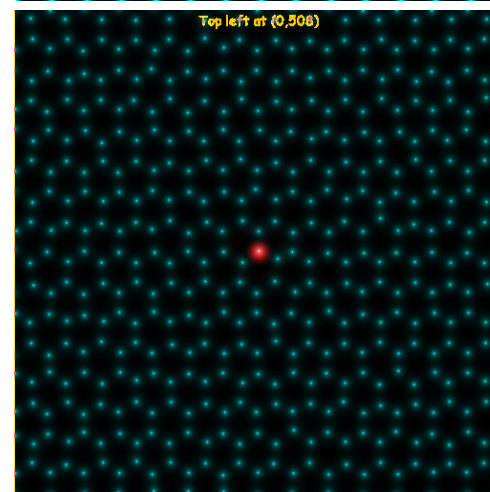
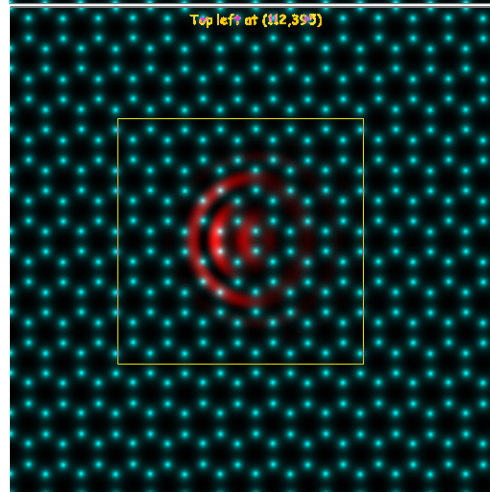
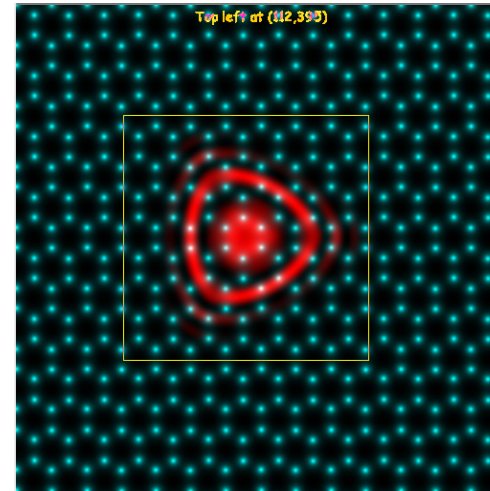
$P(\vec{x})$: source intensity distribution as measured at the sample plane

Aberrations modify the source intensity distribution. STEM scans the corrected probe $P(\vec{x})$ on the crystal entrance plane ($I(\vec{x}) = I_o(\vec{x}) \otimes P(\vec{x})$).

2 fold astigmatism.



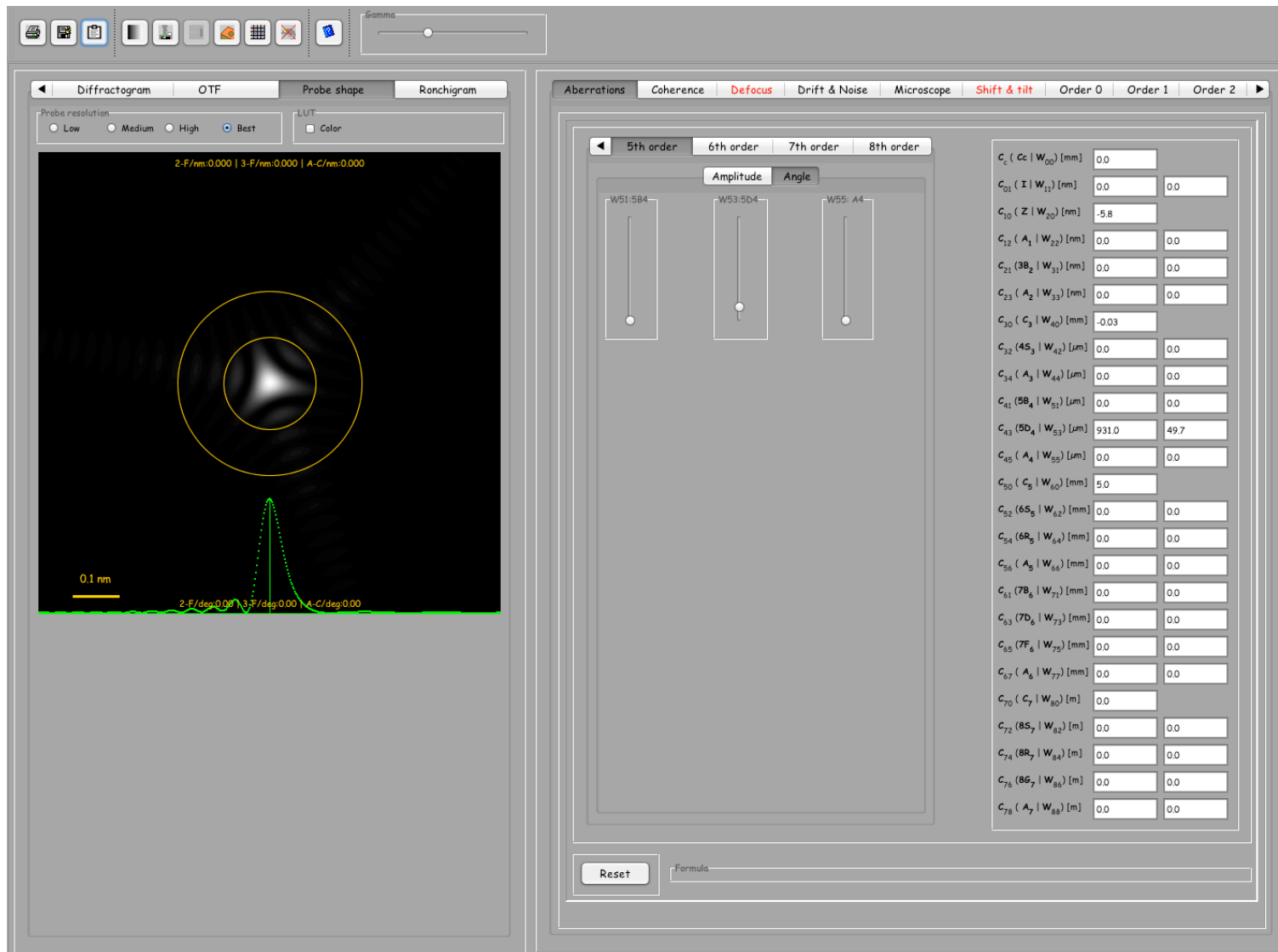
3 fold astigmatism.



Coma.

Corrected probe.

JEMS: STEM probe formation and aberrations



STEM probe with C_{43} geometrical aberration (Krivanek) or W_{53} wavefront aberration or 4th order three-lobe (Haider).

- Dynamical scattering.
- Optical system.
- —→ **Comparing HRTEM and HRSTEM.**

Wavefront aberrations to 6th order (cartesian coordinates)

$\{z, \pi(u^2 + v^2)\lambda\}$ (*defocus*)

$\{W(1, 1), 2\pi(u \cos(\phi(1, 1)) + v \sin(\phi(1, 1)))\}$

$\{W(2, 2), \pi\lambda((u - v)(u + v) \cos(2\phi(2, 2)) + 2uv \sin(2\phi(2, 2)))\}$

$\{W(3, 1), \frac{2}{3}\pi(u^2 + v^2)\lambda^2(u \cos(\phi(3, 1)) + v \sin(\phi(3, 1)))\}$

$\{W(3, 3), \frac{2}{3}\pi\lambda^2(u(u^2 - 3v^2) \cos(3\phi(3, 3)) - v(v^2 - 3u^2) \sin(3\phi(3, 3)))\}$

$\{W(4, 0), \frac{1}{2}\pi(u^2 + v^2)^2\lambda^3\}$ (*3rd order spherical aberration or C₃*)

$\{W(4, 2), \frac{1}{2}\pi(u^2 + v^2)\lambda^3((u - v)(u + v) \cos(2\phi(4, 2)) + 2uv \sin(2\phi(4, 2)))\}$

$\{W(4, 4), \frac{1}{2}\pi\lambda^3((u^4 - 6v^2u^2 + v^4) \cos(4\phi(4, 4)) + 4u(u - v)v(u + v) \sin(4\phi(4, 4)))\}$

$\{W(5, 1), \frac{2}{5}\pi(u^2 + v^2)^2\lambda^4(u \cos(\phi(5, 1)) + v \sin(\phi(5, 1)))\}$

$\{W(5, 3), \frac{2}{5}\pi(u^2 + v^2)\lambda^4(u(u^2 - 3v^2) \cos(3\phi(5, 3)) - v(v^2 - 3u^2) \sin(3\phi(5, 3)))\}$

$\{W(5, 5), \frac{2}{5}\pi\lambda^4(u(u^4 - 10v^2u^2 + 5v^4) \cos(5\phi(5, 5)) + v(5u^4 - 10v^2u^2 + v^4) \sin(5\phi(5, 5)))\}$

$\{W(6, 0), \frac{1}{3}\pi(u^2 + v^2)^3\lambda^5\}$ (*5th order spherical aberration or C₅*)

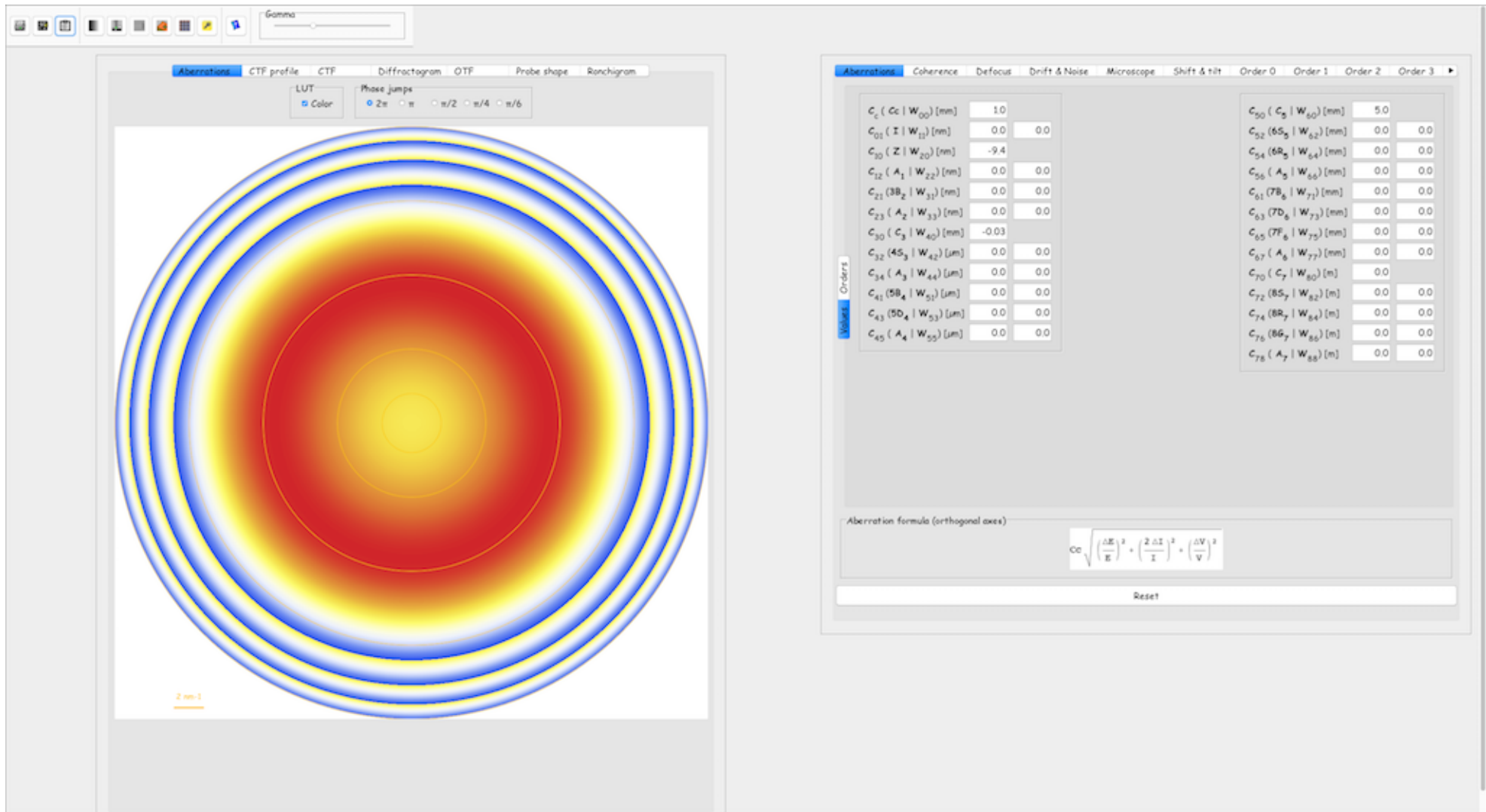
$\{W(6, 2), \frac{1}{3}\pi(u^2 + v^2)^2\lambda^5((u - v)(u + v) \cos(2\phi(6, 2)) + 2uv \sin(2\phi(6, 2)))\}$

$\{W(6, 4), \frac{1}{3}\pi\lambda^5((u^6 - 5v^2u^4 - 5v^4u^2 + v^6) \cos(4\phi(6, 4)) + 4uv(u^4 - v^4) \sin(4\phi(6, 4)))\}$

$\{W(6, 6), \frac{1}{3}\pi\lambda^5((u^6 - 15v^2u^4 + 15v^4u^2 - v^6) \cos(6\phi(6, 6)) + 2uv(3u^4 - 10v^2u^2 + 3v^4) \sin(6\phi(6, 6)))\}$

JEMS describes wavefront aberrations to order 8. And provides a dictionary of equivalent notation:


Wave-front aberrations to order 8




Wavefront aberrations up to order 8 can be introduced in HRTEM image formation and HRSTEM probe formation.

Aberrations dictionary (order 8)

$C_c (C_c W_{00})$ [mm]	1.0	
$C_{01} (I W_{11})$ [nm]	0.0	0.0
$C_{10} (Z W_{20})$ [nm]	-9.4	
$C_{12} (A_1 W_{22})$ [nm]	0.0	0.0
$C_{21} (3B_2 W_{31})$ [nm]	0.0	0.0
$C_{23} (A_2 W_{33})$ [nm]	0.0	0.0
$C_{30} (C_3 W_{40})$ [mm]	-0.03	
$C_{32} (4S_3 W_{42})$ [μm]	0.0	0.0
$C_{34} (A_3 W_{44})$ [μm]	0.0	0.0
$C_{41} (5B_4 W_{51})$ [μm]	0.0	0.0
$C_{43} (5D_4 W_{53})$ [μm]	0.0	0.0
$C_{45} (A_4 W_{55})$ [μm]	0.0	0.0
$C_{50} (C_5 W_{60})$ [mm]	5.0	
$C_{52} (6S_5 W_{62})$ [mm]	0.0	0.0
$C_{54} (6R_5 W_{64})$ [mm]	0.0	0.0
$C_{56} (A_5 W_{66})$ [mm]	0.0	0.0
$C_{61} (7B_6 W_{71})$ [mm]	0.0	0.0
$C_{63} (7D_6 W_{73})$ [mm]	0.0	0.0
$C_{65} (7F_6 W_{75})$ [mm]	0.0	0.0
$C_{67} (A_6 W_{77})$ [mm]	0.0	0.0
$C_{70} (C_7 W_{80})$ [m]	0.0	
$C_{72} (8S_7 W_{82})$ [m]	0.0	0.0
$C_{74} (8R_7 W_{84})$ [m]	0.0	0.0
$C_{76} (8G_7 W_{86})$ [m]	0.0	0.0

Notation 

Formula 

7th order chapelet aberration (C76::W86::8G7)

$$\frac{1}{8} \lambda^7 ((u^8 - 14 u^6 v^2 + 14 u^2 v^6 - v^8) \cos[6 \phi_{86}] + 2 u v (3 u^6 - 7 u^4 v^2 - 7 u^2 v^4 + 3 v^6) \sin[6 \phi_{86}])$$

Equivalent aberration notation (Krivanek, Rose/Haider, wave-front aberrations).

HRTEM

coherent or partially coherent image formation process with coherent or partially coherent incident wave.

TEM ($\tilde{T}(\vec{q})$: **T**ransfer **F**unction):

$$\tilde{\Psi}_i(\vec{q}) = \tilde{\Psi}_o(\vec{q}) \tilde{T}(\vec{q})$$

$$\Psi_i(\vec{x}) = \int \tilde{\Psi}_o(\vec{q}) \tilde{T}(\vec{q}) e^{2\pi i \vec{q} \cdot \vec{x}} d\vec{q}$$

HRSTEM

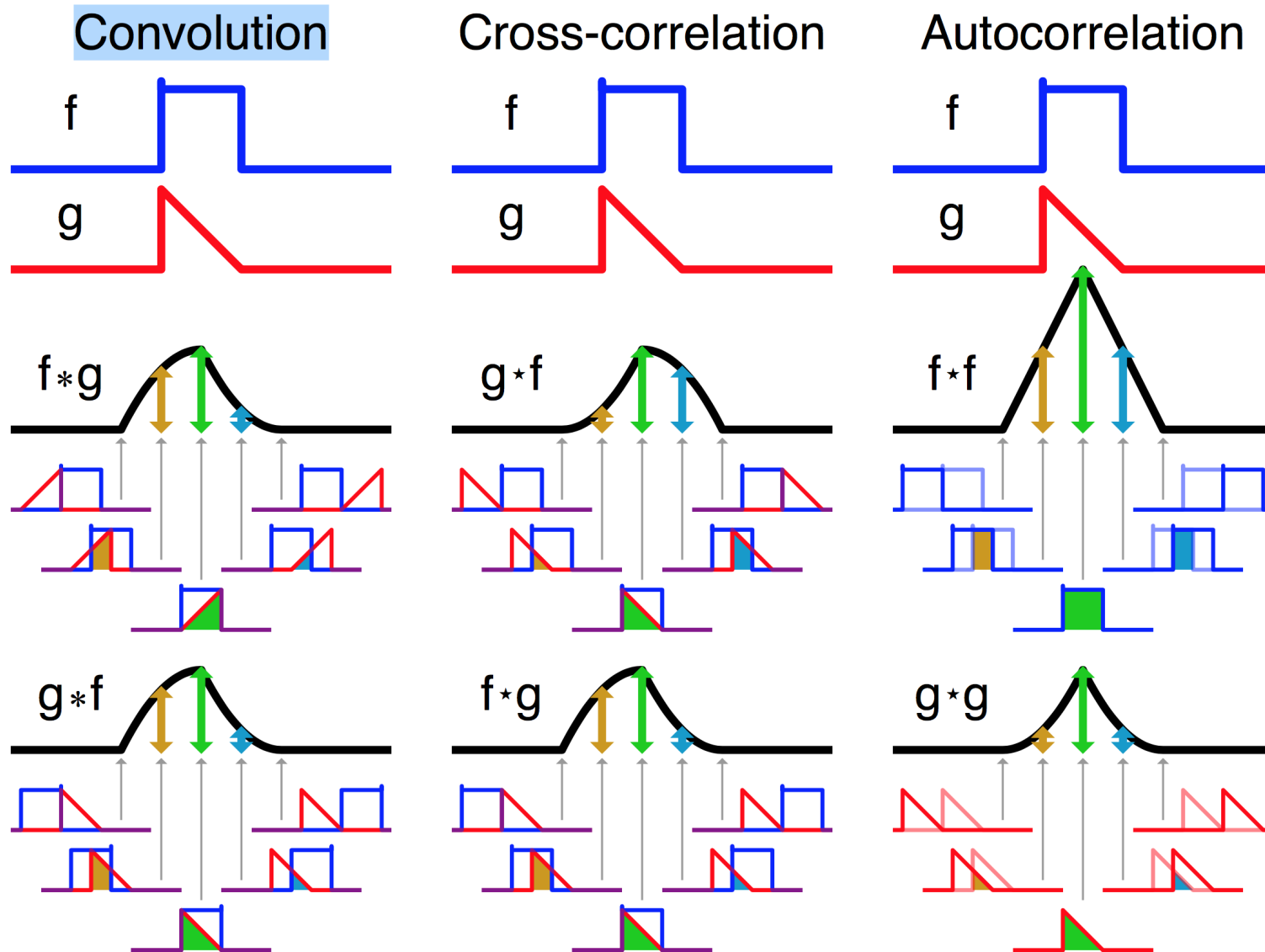
Incoherent image formation process with coherent or partially coherent probe.

STEM ($\widetilde{OTF}(\vec{q}) = \tilde{T}(\vec{q}) \otimes \tilde{T}(-\vec{q})$: **O**ptical **T**ransfer **F**unction):

$$\begin{aligned}
 I(\vec{x}) &= \langle \Psi_i(\vec{x}; t) \Psi_i^*(\vec{x}; t) \rangle && \text{(time average)} \\
 \Psi_i(\vec{x}; t) &= \Psi_o(\vec{x}; t) \otimes T(\vec{x}) && (T(\vec{x}) : \text{PSF independent of } t) \\
 I(\vec{x}) &= \langle [\Psi_o(\vec{x}; t) \otimes T(\vec{x})] [\Psi_o^*(\vec{x}; t) \otimes T^*(\vec{x})] \rangle && (\otimes \text{ convolution.}) \\
 I(\vec{x}) &= [T(\vec{x}) T^*(\vec{x})] \otimes \langle \Psi_o(\vec{x}; t) \Psi_o^*(\vec{x}; t) \rangle && (T(\vec{x}) \text{ is time independent.}) \\
 \langle \Psi_o(\vec{x}; t) \Psi_o^*(\vec{x}; t) \rangle &= |\Psi_o(\vec{x})|^2 && \text{(complete spatial incoherence)} \\
 I(\vec{x}) &= |\Psi_o(\vec{x})|^2 \otimes [T(\vec{x}) T^*(\vec{x})] \\
 I(\vec{x}) &= I_o(\vec{x}) \otimes [T(\vec{x}) T^*(\vec{x})] = I_o(\vec{x}) \otimes P(\vec{x}) && (P: \text{probe intensity})
 \end{aligned}$$

Probe function $P(\vec{x})$: source intensity distribution as measured at the sample plane.

Convolution, cross-correlation & autocorrelation



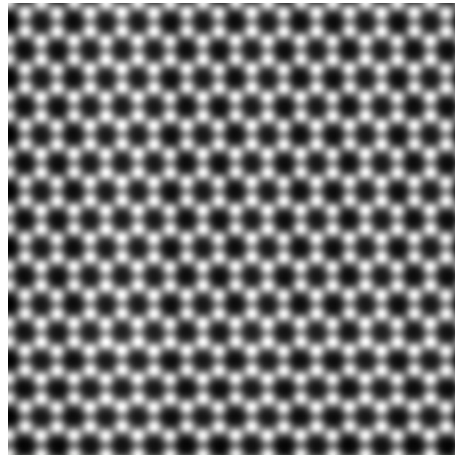
Numerous approximations are involved in calculating $I_0(\vec{x})$ (object intensity):

- Simple **projected potential**: no channeling effect (**W**Weak **O**bject **A**pproximation).
- **Multislice** or **Bloch-wave** calculation: **channeling** + inelastic scattering (absorption or optical potential).
- **Frozen lattice** (phonon) approximation: atoms of super-cell displaced out of equilibrium position, **probe scanned** on imaged area, intensity collected by annular detector. Allows to simulate HAADF (High Angle Annular Dark Field), BF (Bright Field), MAADF (Medium Angle Annular Dark Field), DPC (Differential Phase Contrast), ...
- References: Allen, Ishizuka, Nellist, Pennycook, Rosenauer, van Dyck, Wang.

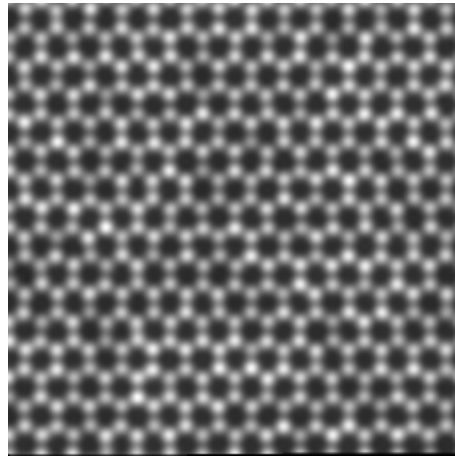
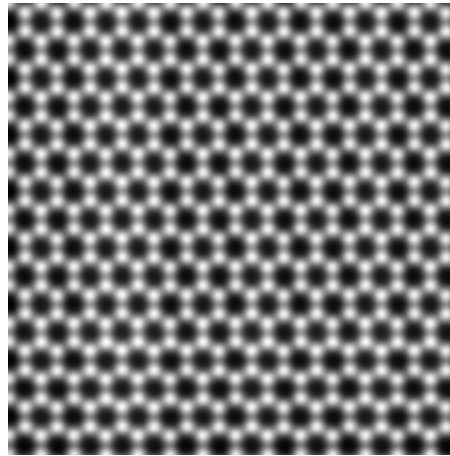
Except the first 2 methods, usually rather long simulation time (faster calculations using GPU).

STEM imaging: graphene

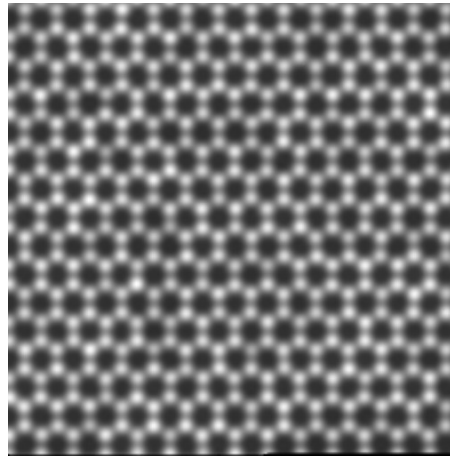
Proj. pot. approx.



Channeling calc.

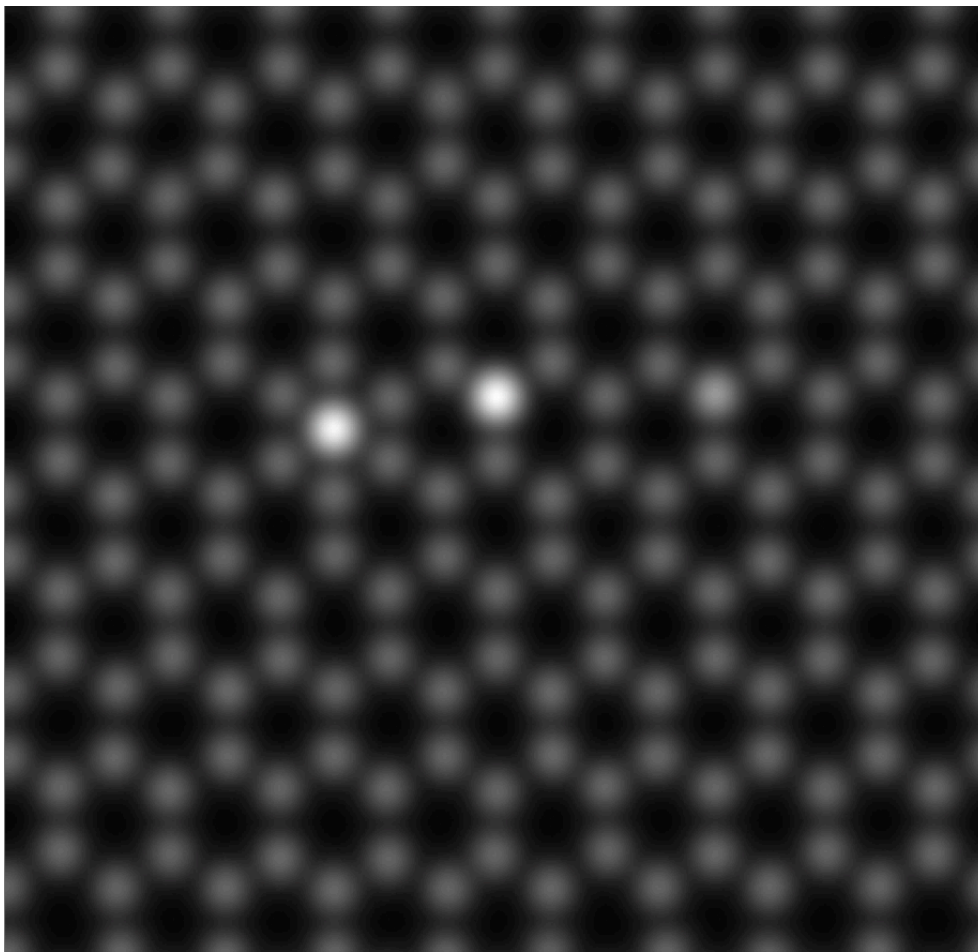


Frozen lattice 5
conf.



Frozen lattice 10
conf.

Frozen lattice: sampling is critical and it is necessary to **repeat the calculation (10 to 40 times)** to image most of the possible atomic configurations.

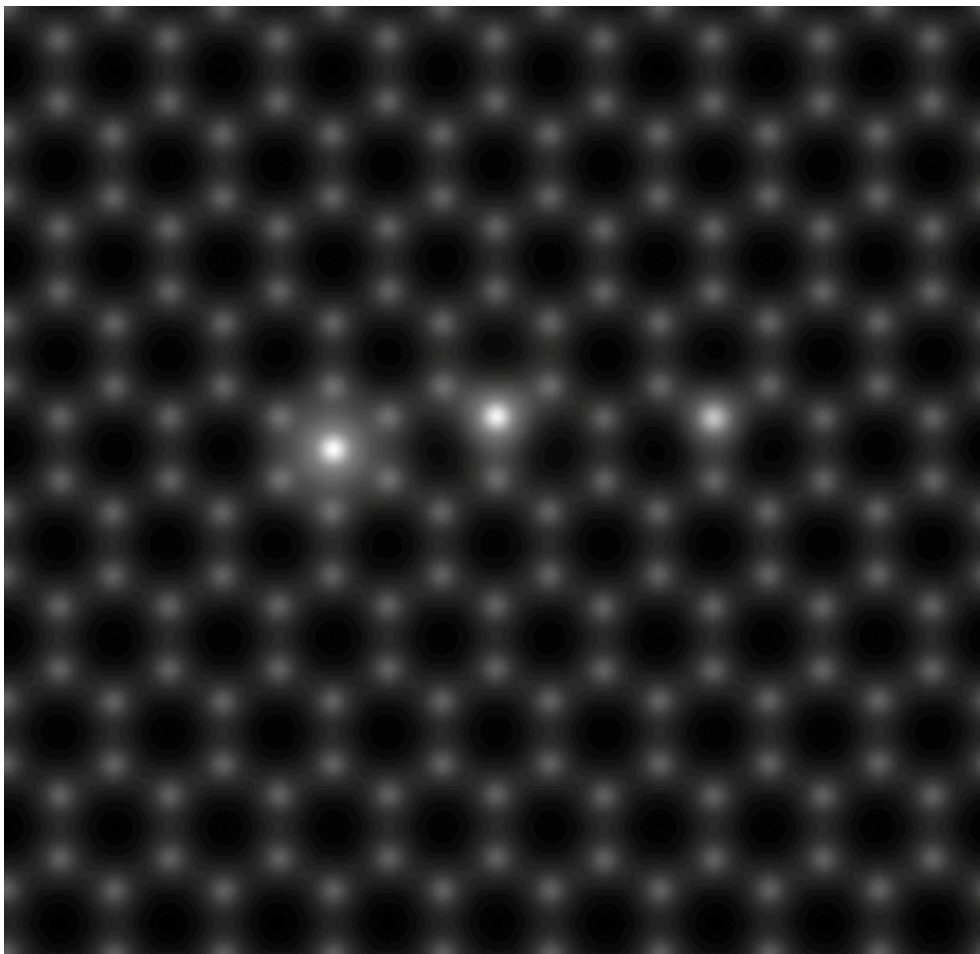


Frozen lattice (~ 400 s).

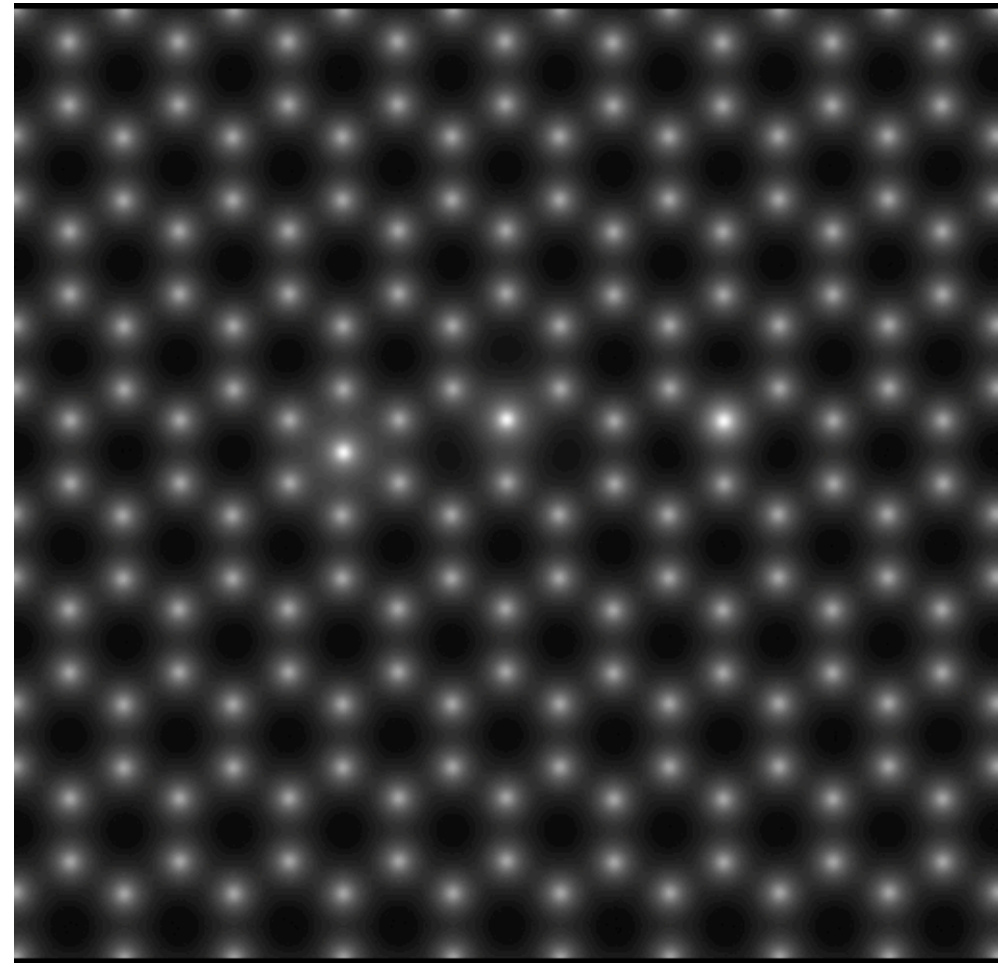


Channeling (~ 2 s).

One Si shows more contrast than 2 C atoms ($i \sim Z^2$) : 14^2 compared to $\sim 2 \times 6^2$.



Weak phase object app., $C_c = 0.5\text{mm}$



Multislice, $C_s = -0.033\text{mm}$, $C_c = 0$, no thermal magnetic noise.

HRTEM does not display the strong contrast difference between one Si and two C as given by HAADF STEM imaging.

HRTEM & HRSTEM image simulations share many calculation methods. Both require precise dynamical calculations that take into account elastic and inelastic electron scattering.

Important difference to remember:

- **HRTEM**: the wave-function $\tilde{W}(\vec{q})$ in the **image** plane is the product of the object wave-function $\tilde{O}(\vec{q})$ with the transfer function of the microscope $\tilde{T}(\vec{q})$:

$$\tilde{W}(\vec{q}) = \tilde{O}(\vec{q}) \times \tilde{T}(\vec{q})$$

- **HRSTEM**: image intensity $I(\vec{x})$ at the **detector position** is the convolution of the object intensity $I_o(\vec{x})$ with the probe intensity $P(\vec{x})$:

$$I(\vec{x}) = I_o(\vec{x}) \otimes P(\vec{x})$$

As a result we can expect a better spatial resolution and no phasing difficulties using HRSTEM.

Thanks for your attention!